CHALMERS
UNIVERSITY OF TECHNOLOGY

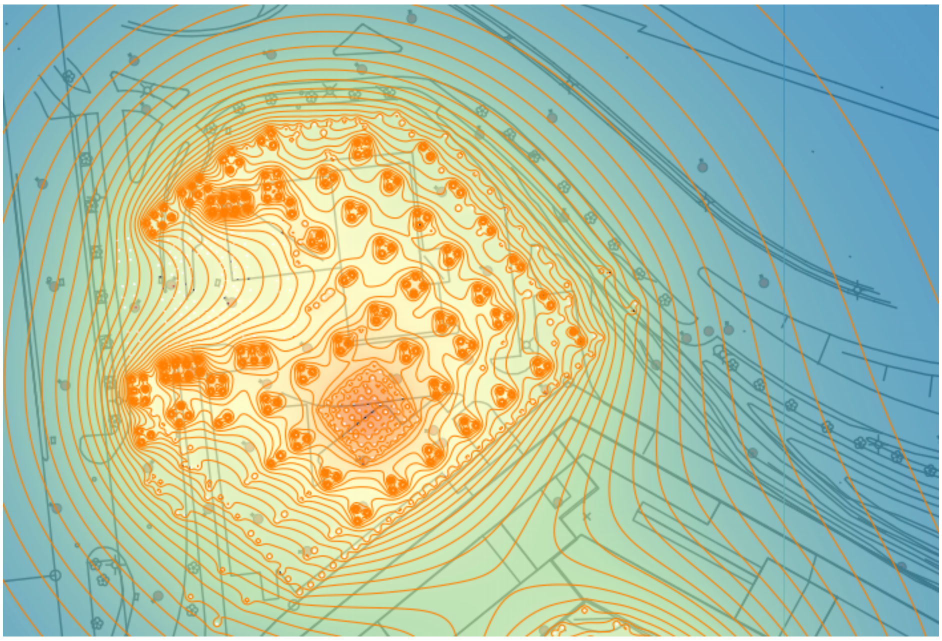

# Prediction of surrounding effects in soft soil deposits due to piling

## A study of comparing different prediction methods

Master's thesis in Infrastructure and Environmental Engineering

TAMER MAAROUF
REBAZ MAHMOUD

Department of Architechture and Civil Engineering
CHALMERS UNIVERSITY OF TECHNOLOGY
Gothenburg, Sweden 2019

Master's thesis ACEX30-19-64

# Prediction of surrounding effects in soft soil deposits due to piling

A study of comparing different prediction methods

TAMER MAAROUF
REBAZ MAHMOUD

Department of Architecture and Civil Engineering
*Division of Geology and Geotechnics*
Chalmers University of Technology
Gothenburg, Sweden 2019

Prediction of surrounding effects in soft soil deposits due to piling
A study of comparing different prediction methods
TAMER MAAROUF
REBAZ MAHMOUD



Supervisor: Norconsult AB and Mats Karlsson
Examiner: Mats Karlsson, Department of Architecture and Civil Engineering

Master's Thesis ACEX30-19-64
Department of Architecture and Civil Engineering
Division of Geology and Geotechnics
Chalmers University of Technology
SE-412 96 Gothenburg
Telephone +46 31 772 1000

Cover: Visualization of vertical displacements obtained with the Shallow Strain Path Method retrieved from ArcGIS, for a project in the area of Gothenburg.

Typeset in LaTeX
Gothenburg, Sweden 2019

Prediction of surrounding effects in soft soil deposits due to piling
Department of Architecture and Civil Engineering
TAMER MAAROUF, REBAZ MAHMOUD
A study of comparing different prediction methods
Chalmers University of Technology

# Abstract

The surrounding effects from pile installation is challenging to predict, and of importance to regard in urban cities like Gothenburg. With deep deposits of soft soil, the requirements on ground improvements in the city are high and can be expensive. In order to reduce the costs for the contractor it is of importance to regard the effect on surrounding soil.

The use of analytical solutions can sometimes be more favourable in order to obtain a first estimate of a geotechnical problem. This since it is time consuming and complex to conduct numerical analysis to a full extent. Therefore, this thesis has focused on the accuracy of the predictions obtained from the Shallow Strain Path method which is an analytical approach. This method was later compared with the outcome from a conducted numerical analysis and measurements from a project located on Hisingen.

The results focuses on the displacements both in the vertical and horizontal direction. The comparison is made with the displacements obtained from the prediction methods, with respect to the distance from pile. Further on, a comparison is made with measurements from a given measurement point. The carried out analyses indicates that the SSPM simple pile solution corresponds best with measurements. The SSPM simple wall is the most deviating method. The two methods line displacement and volume expansion approaches used in the numerical analysis predicts similar behaviour regarding the deformations.

Evaluation of more cases is necessary for validation of the accuracy of the different prediction methods. This in order to suggest a general conclusion regarding which method that could be preferable.

Keywords: Sagaseta, SSPM, SPM, FEM, PLAXIS 2D, Surrounding effects, Soft soil, Piling, Prediction.

## Acknowledgements and disclaimer

We would like to thank our supervisor Mats Karlsson for his encouragement and contribution with expertise throughout the entire process. We would also like to thank the geotechnical division at Norconsult AB for their help regarding practical knowledge concerning Plaxis 2D and SSPM.

Lastly, we would like to express our gratitude towards our families and friends for their support and motivation during our time at Chalmers but also in life.

Disclaimer: The authors and Norconsult AB are not responsible for any consequences and/or damages resulting from the use of the stated conclusions, approaches or any errors given in this report.

Tamer Maarouf & Rebaz Mahmoud, Gothenburg, June 2019

*"I skuggan av hjältar"*

*-Parham Pazooki*

# Contents

# List of Figures

# List of Tables

# Nomenclature

**Abbreviations**

$LE$ Linear Elastic

$MC$ Mohr Coulomb

$OCR$ Over consolidation ratio

$POP$ Pre-overburden pressure

$SS$ Soft Soil

**Greek letters**

$\gamma_{sat}$ Wet unit weight

$\gamma_{unsat}$ Dry unit weight

$\kappa^*$ Modified swelling index

$\lambda^*$ Modified compression index

$\nu'$ Effective Poisson's ratio

$\nu_{ur}$ Poisson's ratio for unloading and reloading

$\phi'$ Friction angle

$\phi'_c$ Friction angle at critical state

$\psi$ Dilatancy angle

$\sigma'_c$ Pre consolidation pressure

$\varepsilon_{vx}$ Volumetric strain in x-direction

**Roman upper case letters**

$E'$ Effective Young's modulus

$E_{oed}$ Oedometer modulus

$G$ Shear modulus

$K_0$ Earth pressure coefficient at rest

$K_0^{NC}$ Earth pressure coefficient for normally consolidated soils

$K_{0x}$ Lateral earth pressure coefficient

$L$ Length of pile

$M_0$ Constant constrained modulus below effective preconsolidation pressure

$R$ Radius of pile

$R_{inter}$ Interface factor

$S$ Point Source - SSPM

$S'$ Mirror image sink - SSPM

$S_t$ Sensitivity

$V$ Volume of pile

$W_L$ Liquid limit

$X_{min}$ Left horizontal boundary

$Y_{min}$ Bottom vertical boundary

**Roman lower case letters**

$c'$ Cohesion intercept

$c_u$ Undrained shear strength

$k_x$ Permeability in horizontal direction

$k_y$ Permeability in vertical direction

$r$ Distance from pile

$r_1$ Width/radius of piling area

$r_2$ New width/radius of piling area

$u_x$ Displacement in the horizontal direction

$u_y$ Displacement in the vertical direction

$w$ Wall thickness

# 1
# Introduction

## 1.1 Background

The installation effects during piling on surrounding soil constitute a major challenge in design in urban areas, like Gothenburg, with deep deposits of soft sensitive clay. Due to its characteristics, the requirements on ground improvement methods used in Gothenburg clay are high. It is of great importance to use installation methods that are affecting the surrounding soil to a minimum extent, due to its relatively high sensitivity (Persson & Stevens, 2012). Ground improvement in Gothenburg can be expensive and of high complexity due to the conditions in the soil. When constructing in the inner city of Gothenburg, the effect on surrounding soil has to be taken in to consideration and described with precision in order to minimize the range of error and to reduce the maintenance and construction cost for the contractor.

Within the field of geotechnical engineering, the use of numerical tools and software has been set as standard procedure due to its ability to model and describe complex soil behavior. The tools are constantly being refined and developed in order to increase the degree of accuracy when conducting such analysis. However, it is of great importance for the user to understand the essence of the quality of the input parameters used in the software as they dictate the quality of the analysis outcome. Using numerical tools can be a time consuming process for complex geotechnical issues, it is therefore in the interest of the industry to sometimes use an analytical method. The use of analytical methods can in some cases be more convenient in order to obtain a first estimation. Norconsult AB has therefore initiated this master thesis in cooperation with the Division of Geology and Geotechnical engineering at the Department Of Architecture and Civil Engineering at Chalmers University Of Technology.

As the city of Gothenburg is growing rapidly, and the use of deep foundations is common, it is necessary to understand and describe the impact on adjacent soil due to installation of piles. This thesis will therefore focus on the use of analytical method Shallow Strain Path Method (SSPM) and numerical modelling in order to obtain adequate displacements in the horizontal and vertical direction. The result from SSPM and the numerical modelling will be compared to measured data from a project located on Hisingen in order to verify the accuracy of the predictions.

## 1.2 Purpose

The purpose of this thesis is to gain a better understanding of how the SSPM can be implemented on pile foundations in soft soil deposits in order to evaluate vertical and horizontal displacements. And further to investigate if there is a possibility to gain adequate results using different prediction methods.

## 1.3 Aim

The aim of this thesis is to analyze how installation of piles in soft clay affects the surrounding soil, and how the SSPM predicts these. The results are later to be compared with numerical analyses using the software Plaxis 2D and measured deformations from field.

## 1.4 Objectives

In order to fulfill the aim of the study the following objectives are to be accomplished:

- Gain knowledge regarding the theory and background of SSPM
- Gain knowledge regarding Plaxis 2D for soft soil deposits
- Model a current project located on Hisingen
- Obtain results regarding vertical and horizontal displacements using SSPM and Plaxis 2D
- Compare the results obtained using SSPM with Plaxis 2D and field measurements
- Find factors that adjusts the predictions of displacement obtained from SSPM compared to field measurements

## 1.5 Limitations

The prediction of effects on surrounding soil caused by piling in in soft soil is a comprehensive subject. There are many factors and mechanisms that affects the prediction, thus following limitations were made in order to limit the scope of the study:

- The thesis will scope a project in soft soil (clay) on Hisingen, Gothenburg.
- Horizontal and vertical displacements on the ground surface will be the main focus.
- Only the initial deformations will be evaluated, hence no time aspect is considered.
- Measurements from field will be available for the piling activities day wise
- No consideration will be taken to workmanship related issues
- No consideration will be given to adjacent piles or buildings in the carried out analysis
- SSPM will be used
- FEM analysis will be used in terms of Plaxis 2D

# 2
# Theory

## 2.1 Pile foundations

Pile foundations are categorized as deep foundations as they transfer the stresses acting on the surface to a considerable depth (Knappett & Craig, 2012). If the conditions of the soil regarding its bearing capacity is critical, piling is an effective method in order to obviate the occurrence of deformations. The use of piles for foundation purposes can be tracked back to the Roman Empire where timber piles were used. Pile foundation is an ancient technique that has been improved through the history of civil engineering (Viggiani, Mandolini, & Russo, 2012). There is a distinction between pile foundation types that are used in different countries due to the different soil conditions, the attitude towards different techniques and the experience amongst engineers in practice.

Piles are classified by their material, installation method, the type of soil they are installed in and the way the piles are loaded (Ahlén, 2009). Timber, steel and concrete are the most common materials used for piles. There are also piles constructed as a combination of materials such as timber and concrete. In Sweden, it is estimated that 75 to 80% of the installed piles are precast driven concrete piles (C. Olsson & Holm, 1993). The installation method and the impact it will have on the pile is the most differentiating factor (Viggiani et al., 2012). The most common installation methods for displacement piles are driving, screwing or pushing. The other category which includes replacement piles involves techniques such as boring or drilling.

### 2.1.1 Displacement Piles

During installation, displacement piles disturbs the surrounding soil and enhances deformations. As penetration of soil occurs, there will be a build up of stresses since the piles are forced into the ground with no precautions. Belonging to the displacement piles are the precast concrete piles and driven steel piles to mention two (Knappett & Craig, 2012). As mentioned before, the most common method for installing piles are driving. This involves a process where the impact of an hammer drives the pile down into the ground, such piles are referred to as driven piles (Viggiani et al., 2012).

### 2.1.2 Replacement piles

Piles installed after soil has been removed, in order to reduce the soil displacement, is referred to as replacement piles (Viggiani et al., 2012). Depending on the purpose of the pile there are several ways of installing one, one method is to cast concrete in the cylindrical void that has been created. Most of the related issues with the replacement piles is the way of creating the shaft where the pile later is to be placed in. This can be done with by either boring or drilling, which are two popular methods that can be enlarged with different alternatives.

Both replacement and displacement piles are methods favoured for different situations, depending on for instance the urban environment and on-site conditions. Since the displacement piles often comes prefabricated they are easy to install, but resulting in high deformations. These piles should be used with precaution in urban environments with present sensitive structures close to the piling area. Unlike the displacement piles, the replacement piles results in less deformations and can be more favoured in urban workplaces. But an aspect to regard is again the on-site conditions. If it is not possible to cast concrete piles on-site then they will not be efficient from a practical point of view (Knappett & Craig, 2012).

## 2.2 Effects due to pile penetration

Deformation of soil will develop laterally and as heave during pile installation. The lateral displacements are present at a given depth, which is difficult to monitor, whereas heave occurs on the ground surface and is easier to detect (Hagerty & Peck, 1971). Hagerty and Peck (1971) concluded that the occurring heave during pile installation in fine-grained soil such as clay, is much less than if the soil composition would be the opposite. If the clay is sensitive, the magnitude of heave occurring on the ground surface is less than if the clay is insensitive due to its incompressible behaviour.

The magnitude of the displacements are related to the pile geometry (diameter and length), the amount of piles installed, stratigraphy, properties of the soil material such as sensitivity and shear strength, and hydraulic conditions. If the piles are installed close to each other, the adjacent soil loses its shear strength and the occurrence of displacements are increased due the increase of compressibility (Zeevaert, 1983). Stratigraphy is of importance when evaluating the effects from a pile group. If the piles in the pile group that constitutes the foundation are located in an area with great elevation variances, the soil will prefer to displace laterally from the higher elevated area towards the lower (Hagerty & Peck, 1971). The occurring heave may be reduced by using pre-boring methods for the piles (Zeevaert, 1983).

When piles penetrates low-permeable clay, an increase of excess pore pressure, which changes the effective stress state, occurs due to the change in void ratio (Dijkstra, Broere, & Heeres, 2011). The state of the soil, initially after an increase of total stress due to an increase of excess pore pressure, is described as undrained conditions (Knappett & Craig, 2012). By initiating undrained conditions, the initial volume of the displaced soil due to pile installation is set to be approximately equal to the volume of the installed pile (Zeevaert, 1983). As the effective stress state changes due to the increase of pore pressure, a reduction may be caused of the stiffness and strength of the penetrated soil (Dijkstra et al., 2011).

Based on the numerical analysis carried out by Massarsch and Wersäll (2013) using finite element method, the maxmium surface heave occurs at a distance between 0.3 to 1 times the pile length. However, heave is still of interest beyond the range of 0.3 to 1.00 times the pile length as it occurs at a distance of four pile lengths but with a less magnitude. Regarding lateral displacements of a single pile, Massarsch and Wesäll (2013) concluded that soil tends to displace in the lateral direction within a zone of three pile lengths.

## 2.3 Strain Path Method

The Strain Path Method (SPM) provides analytical approximations of displacements due to piling in clays (Baligh, 1985). The method is advantageous in comparison with other approaches, such as the Cavity expansion method, since it considers both horizontal and vertical displacements.

The method was developed by conducting many laboratory and field observations when installing different rigid objects in soils. It was found that the penetration process could be reduced to a flow problem, were soil particles flow around a penetrating object (Baligh, 1985). This could be done since SPM assumes that the deformations and strains for deep penetration problems are dominated by kinematic constraints. In order to use this approach SPM assumes that penetration occurs under quasi-static steady state conditions, and that the soil is isotropic, homogeneous, incompressible, non-viscous and rate dependent. The method also comprises that the stress conditions should be isotropic and that there are no roughness at the interface between the soil and pile. Baligh (1985) stated that the assumptions are to be considered as vital in order to perform the SPM correctly.

In order to obtain the strains using the SPM, numerical integration of a velocity field around the pile is required (Baligh, 1985). The velocity field is achieved with the same potential flow theory used in fluid dynamics, which implies to combine sources and sinks with a uniform flow field in a given space domain. This field arises from the soil, therefore the assumption about incompressibility includes conservation of volume.

The effective stresses can later on be calculated using any effective stress based constitutive model. This is implied for the discrete points where the strains paths already have been obtained (Eulerian approach). By following the procedure proposed by SPM, it can be stated that the method separates the kinematic process and the mechanical response of the soil. Since the stress state is considered to be isotropic, the calculated effective stresses will not satisfy all the equilibrium conditions, therefore small errors will still remain (Baligh, 1985).

## 2.4 Shallow Strain Path Method

The Shallow Strain Path Method (SSPM) presented by Sagaseta et al. (1997) is a method for solving deep penetration problems based on the SPM. The main difference is that the effects of the ground surface is incorporated in the solutions but also, the reference system for SSPM is not fixed to the penetrating object. With the presence of the ground surface, the penetration is no longer a steady state process. Thus, SSPM considers a source which penetrates downwards from a free surface (Sagaseta et al., 1997). The complexity of the method is, as in the SPM, still formulated in terms of velocities and strain rates. When obtained for the three steps as seen in figure 2.1, numerical integration along the particle path will provide large strain solutions for the penetration problem. An important statement is that the corrective shear tractions along the surface in step three (see figure 2.1) are obtained by small strain elastic solutions. By implementing the procedure described in step 3, an approximation of the deformations of soil elements close to the surface and the penetrating object are obtained.

In order to use SSPM for prediction of displacements due to piling of a pile group, super positioning of the piles has to be made in to one super pile. This as SSPM only calculates the deformation for one pile. When using super positioning principle for a set of piles, the super-pile is placed in the centre of the pile group (Edstam & Kullingsjö, 2011). The area of the super-pile is set equal to the total area of the piles included in the pile group. According to Edstam and Kullingsjö (2011), the use of a super-pile should not be implemented to evaluate ground displacement close to an individual pile nor between piles. Hence, the technique may be used if the location of the displacements that are to be assessed are at a sufficient distance from the pile.

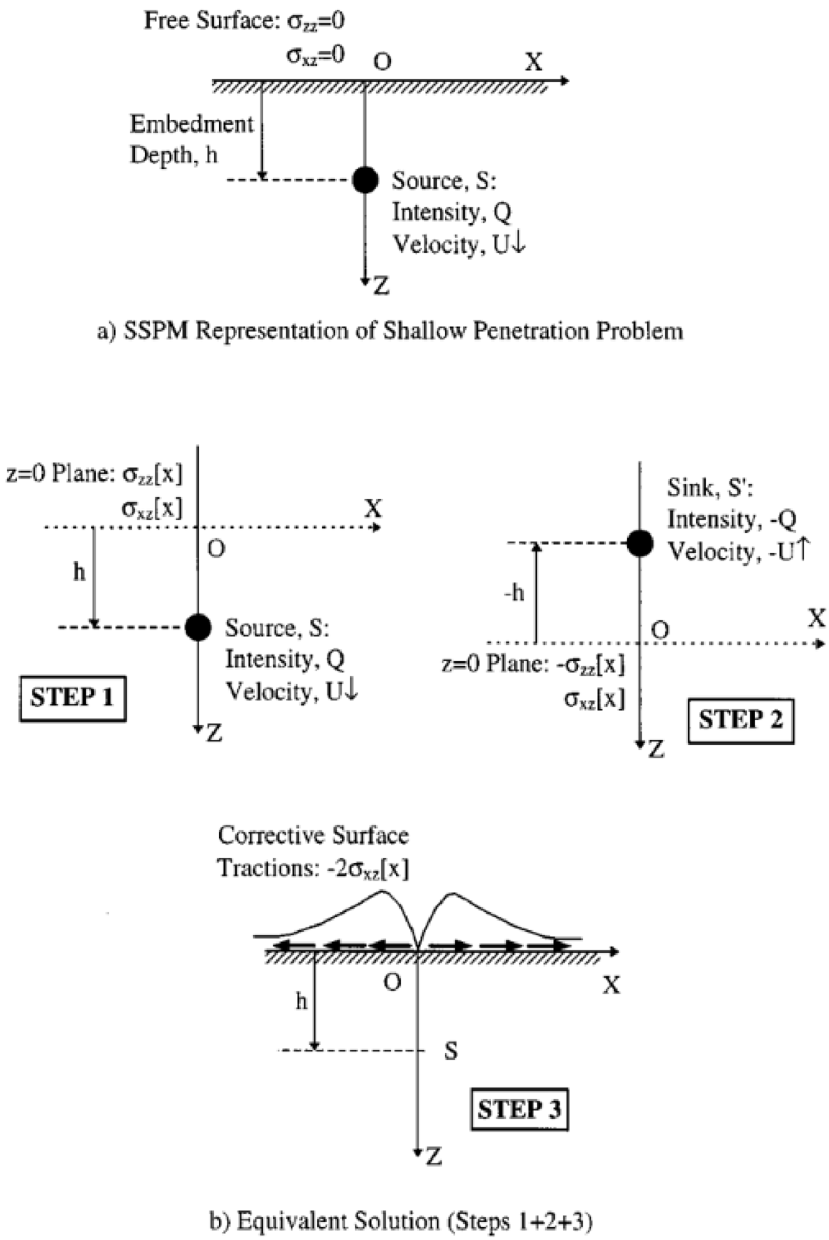


**Figure 2.1:** Conceptual model of SSPM for stress free surface (Sagaseta et al., 1997).

The three steps in the figure above generates three components: 1) Source S, 2) Sink S', 3) Corrective shear tractions, the velocities and strain rates are given as the sum of these. Equation 2.1 shows how the displacements can be obtained by integrating the velocities along the particle path. Where $(x, z)$ is the final position of a particle, that was initially located at $(x_0, z_0)$ when the penetrating source is at a depth h.

$$\begin{Bmatrix} x(h) \\ z(h) \end{Bmatrix} = \begin{Bmatrix} x_0 \\ z_0 \end{Bmatrix} + \int_0^t \begin{Bmatrix} v_x(x,z,h) \\ v_z(x,z,h) \end{Bmatrix} dt = \begin{Bmatrix} x_0 \\ z_0 \end{Bmatrix} + \int_0^h \begin{Bmatrix} v_x(x,z,h) \\ v_z(x,z,h) \end{Bmatrix} \frac{1}{U} dh \tag{2.1}$$

Integration of the strain rates along the particle path according to equation 2.2 gives the strains.

$$\varepsilon_{ij} = \int_0^t \dot{\varepsilon}_{ij}(x, z, h)dt = \int_0^h \frac{1}{U}\dot{\varepsilon}_{ij}(x, z, h)dh \tag{2.2}$$

When assuming small strain conditions, the solution for equation 2.1 can be simplified. In the expression, $(v_x, v_z)$ can be replaced by the initial coordinates $(x_0, z_0)$. By using this assumption the solution can be expressed in closed form for different penetrometers. For a simple wall, the expression is simplified to equation 2.3 and 2.4.

$$\delta_{xSS} = \frac{w}{\pi}\left[\tan^{-1}\left(\frac{z+L}{x}\right) - \tan^{-1}\left(\frac{z-L}{x}\right) + 2xz\left(\frac{1}{r_2^2} - \frac{1}{x^2+z^2}\right)\right] \tag{2.3}$$

$$\delta_{zSS} = -\frac{w}{\pi}\left[\ln\left(\frac{r_1 r_2}{x^2+z^2}\right) - 2z\left(\frac{z+L}{r_2^2} - \frac{z}{x^2+z^2}\right)\right] \tag{2.4}$$

Different coordinates are used depending on the penetrometer geometry, and the approach of solving the problem either using axisymmetric or plane strain assumption. Figure 2.2 shows the coordinate axis that is used for a simple wall, simple pile and a simple open tube. In combination with assuming small strain conditions and only considering deformations at ground surface, SSPM can be reduced to the following expressions:

For simple wall:

$$\delta_{xSS}(x, 0) = 2\frac{w}{\pi}\tan^{-1}\left(\frac{L}{x}\right) \tag{2.5}$$

$$\delta_{zSS}(x, 0) = -\frac{w}{\pi}\ln\left[1 + \left(\frac{L}{x}\right)^2\right] \tag{2.6}$$

For simple pile:

$$\delta_{rSS}(r, 0) = \frac{R^2}{2}\frac{L}{r\sqrt{r^2+L^2}} = \frac{\Omega}{2\pi}\frac{L}{r\sqrt{r^2+L^2}} \tag{2.7}$$

$$\delta_{zSS}(r, 0) = -\frac{R^2}{2}\left(\frac{1}{r} - \frac{1}{\sqrt{r^2+L^2}}\right) = -\frac{\Omega}{2\pi}\left(\frac{1}{r} - \frac{1}{\sqrt{r^2+L^2}}\right) \tag{2.8}$$

For the simple open tube:

$$\delta_{rSS}(0, 0) = 0 \tag{2.9}$$

$$\delta_{zSS}(0, 0) = -2wR\left(\frac{1}{R} - \frac{1}{\sqrt{R^2+L^2}}\right) = -\frac{\Omega}{2\pi}\left(\frac{1}{R} - \frac{1}{\sqrt{R^2+L^2}}\right) \tag{2.10}$$

The deformations can only be estimated in the centre of the tube and at the ground surface if equations 2.9 and 2.10 are used. It is also of importance to only apply this for open-ended piles that are not plugged.

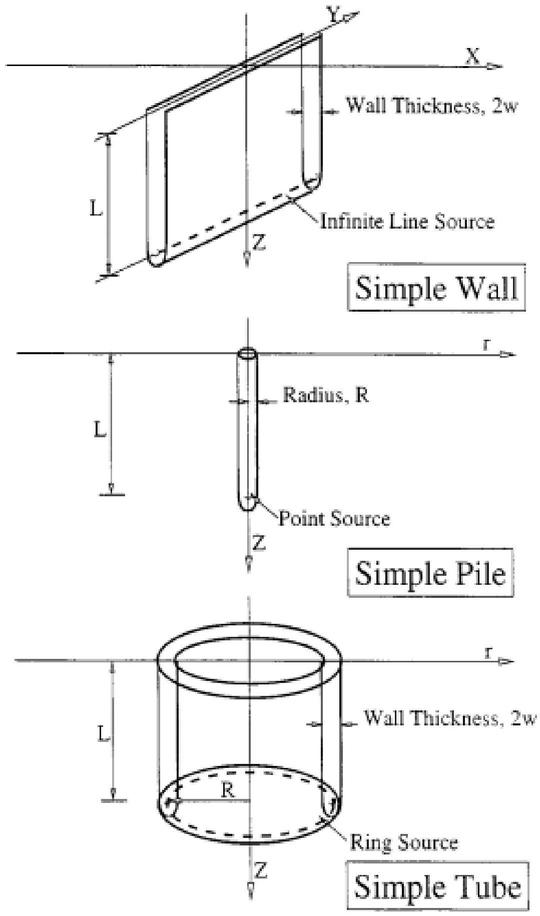


**Figure 2.2:** Co-ordinate frames for the different penetrometer geometries (Sagaseta et al., 1997).

## 2.5 Material models in Plaxis

Several constitutive models and theories have been developed and formulated in order to capture the behaviour of soil. Still, there are not an existing formulation that can capture the right behaviour from all aspects due to the complex properties of soils (Brinkgreve, 2002). Different soils tends to behave differently which is a limitation when using constitutive models as they may be more suitable for one soil type than another, depending on the model used. The constitutive model chosen for interpreting a problem should therefore correspond to right parameters and model, as the input will determine the quality of the outcome. The following three material models are presented in this section: Linear Elastic, Mohr-Coulomb and Soft Soil.

### 2.5.1 Linear elastic model

The linear elastic material model (LE-model), is the simplest material model available for soil modelling in Plaxis. The formulation of the material model is derived from Hooke´s law of isotropic linear elastic behaviour (Brinkgreve, 2002). The parameters necessary when using the LE-model are the effective Young's modulus ($E'$) and the effective Poisson's ratio ($\nu'$). Additionally, it is possible to add the oedemoter modulus ($E_{oed}$) and the shear modulus ($G$). However, by using $E_{oed}$ and $G$, $E'$ and $\nu'$ are changed accordingly. The LE-model is often unfeasible for soil modelling due to the assumption of linear elasticity as soil behaviour is non-linear and irreversible. The use of the LE-model is of interest when modelling structures of certain materials and properties such as concrete plates and walls but it can also be used when modelling bedrock. When using the LE-model the stress state is not limited which causes issues during modelling as strength will be infinite (Karstunen et al., 2017). Care must therefore be taken when modelling geotechnical issues using LE, as failure will not occur.

### 2.5.2 Mohr Coulomb model

The Mohr-Coulomb model (MC-model) is often defined as linear elastic perfectly plastic. This involves the theory of the LE model (Hooke's law of isotropic linear elastic behaviour) in combination with a plastic part which is defined by Coloumb's law (Jia, 2018). Since plasticity involves irreversible strains, it is of interest to evaluate whether plastic strains will occur or not. This is done by introducing a yield function based on Mohr-Coulomb's failure criterion. Since the model is perfectly plastic no stress state above the failure envelope is allowed. States of stress represented by points under the failure line (i.e in the yield surface) will result in elastic strains. Plastic strains will occur only if the achieved stress state reaches the Mohr-Coulomb failure line see figure 2.3 (Brinkgreve et al., 2017).

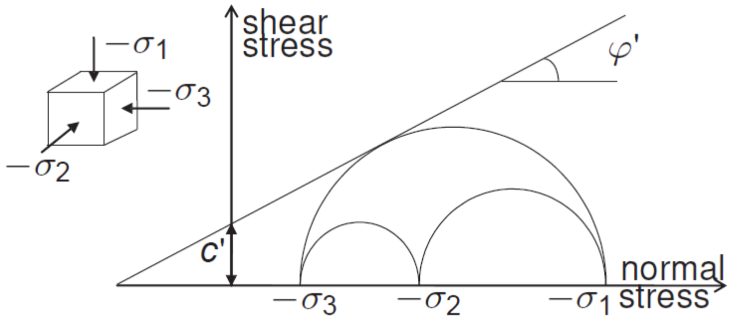


**Figure 2.3:** Mohr-Coulomb's failure line (Brinkgreve et al., 2017).

In comparison with Linear Elastic model this one involves two more parameters, the friction angle ($\phi'$) and the cohesion intercept ($c'$). Other parameters defined in the LE model is still of interest in order to model the elastic region of MC. It is of importance to comprehend that the MC-model is not fully representing real soil behaviour and is according to Karstunen et al. (2017) not suitable for normally or lightly overconsolidated soils. Therefore, the MC-model is not considered as an advanced one and is often used to only get a first approximation.

### 2.5.3 Soft Soil model

The Soft Soil model (SS-model) is not considered as a Critical State Model but it is classified as an advanced material model (Brinkgreve et al., 2017). In comparison to the LE-model and MC-model, the SS-model does not assume linear relationship between strain and stress during primary loading, instead it uses a hyperbolic relationship. The yield surface is an ellipse and the size of it is determined by the over consolidation ratio (OCR) or the pre-overburden pressure (POP). OCR and POP are depending on the geological history of soil in terms of apparent preconsolidation pressure ($\sigma_c'$). Hence, caution is required during interpretation of $\sigma_c'$-values due to the SS-models' sensitivity towards OCR and POP (Karstunen et al., 2017).

The shape of the yield surface is an ellipse in comparison to the Modified Cam Clay material model. With the adjusted yield surface, the model is able to give a good $K_0$-prediction at the normally consolidated region. By using the adjusted yield surface a separate failure condition has to be initiated, this is made by assuming Mohr Coulomb failure (Karstunen et al., 2017). However, the possible stress states that are obtainable in the SS-model are restricted by the Mohr Coulomb failure criterion, hence the model does not account for strain softening. By using Mohr Coulomb failure criterion the model assumes a constant friction angle. The failure criterion can be expressed as equation 2.11

$$f_f = \frac{1}{2}\left(\sigma_3' - \sigma_1'\right) + \frac{1}{2}\left(\sigma_3' + \sigma_1'\right) sin\phi_c' \tag{2.11}$$

where $\phi_c'$ is the friction angle at critical state. The model also allows non-linear stiffness which is beneficial when conducting deformation analysis (Karstunen et al., 2017). The critical state parameter M is not used for failure in the SS-model. However, M* is used to modify the height of the ellipse and thereby it is directly affecting the shape of the yield surface (Brinkgreve et al., 2017)(see figure 2.4).

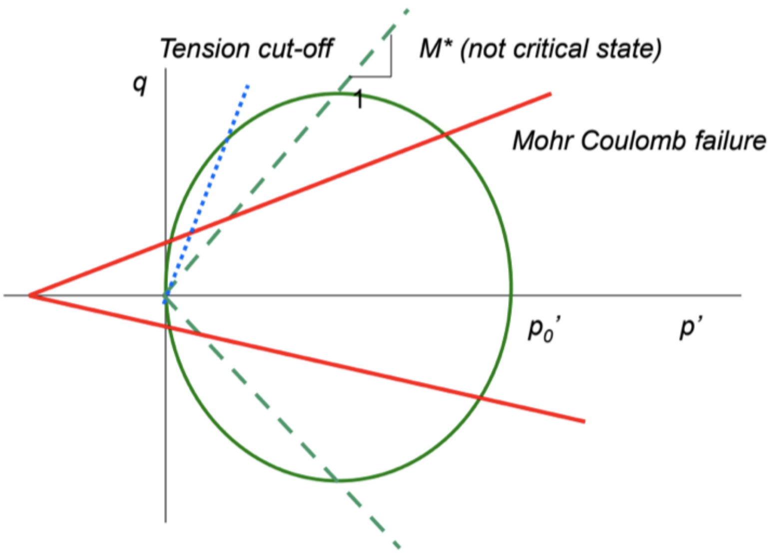


**Figure 2.4:** Soft soil model including its adoption of Mohr Coulomb failure line (Karstunen et al., 2017).

The SS-model uses modified compression index ($\lambda^*$) and modified swelling index ($\kappa^*$) using natural logarithm which enhances a non-linear elasticity in comparison to the MC-model. In order to describe the elastic behaviour when using the SS-model not only $\kappa^*$ is required, Poisson's ratio for unloading/reloading ($\nu_{ur}'$) is also necessary (Karstunen et al., 2017).

As stated by Karstunen et al.(2017), anisotropic consolidated undrained triaxial compression (CAUC) and constant rate of strain (CRS) are necessary to perform when modelling using the SS-model. An analysis may be carried out with the results given by CRS-test only, which is common in Sweden. However, knowledge regarding the local friction angle at critical state is crucial. The impact from OCR on the outcome of the analysis should also be evaluated when data obtained from CRS testing is the source of parameters.

## 2.6 Numerical modelling in Plaxis 2D

In this section, the importance of the geometry settings are highlighted. The modelling methods of piles, as well the surrounding effects are introduced and considerations are presented. Finally the mindset regarding the impact from several piles will be mentioned briefly.

### 2.6.1 Geometry

In order to design a representative model of a real case it is of importance to understand how to put up the geometry in Plaxis. This becomes vital when 2D software is used for 3D problems, in order to downscale the scenario, assumptions must be made considering the geometry. The software Plaxis 2D offers two options, those are presented below.

#### 2.6.1.1 Axisymmetry

By using the Axisymmetric option in Plaxis 2D the model will adopt a specific design. This alternative is most common for circular structures with a uniform radial cross section (Brinkgreve et al., 2017), where the model will form a circular shape around the y-axis (see figure 2.5). The user works in the cross section limited by the y and x-axis, but the software will consider the out of plane direction (z-axis) by assuming that the all strains are equal in the radial direction $\varepsilon_x = \varepsilon_z$ (Tjie-liong, 2015).

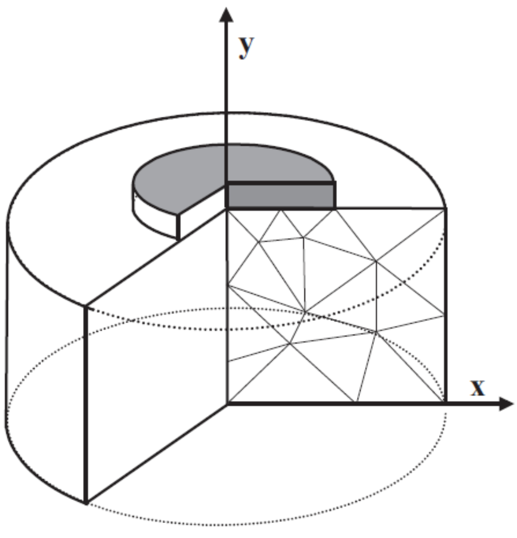


**Figure 2.5:** Visualization of the Axisymmetric model in Plaxis 2D (Brinkgreve et al., 2011).

#### 2.6.1.2 Plane Strain

For scenarios with a uniform cross section in the perpendicular out of plane direction (z-axis), the plane strain option can be chosen (Brinkgreve et al., 2011). This is often used for road banks or sprawled excavations where the length is larger than the width (Tjie-liong, 2015). This geometry corresponds well with a stress state and loading scheme that is uniform along the stretch and therefore the cross section in x-y will be representative (see figure 2.6).

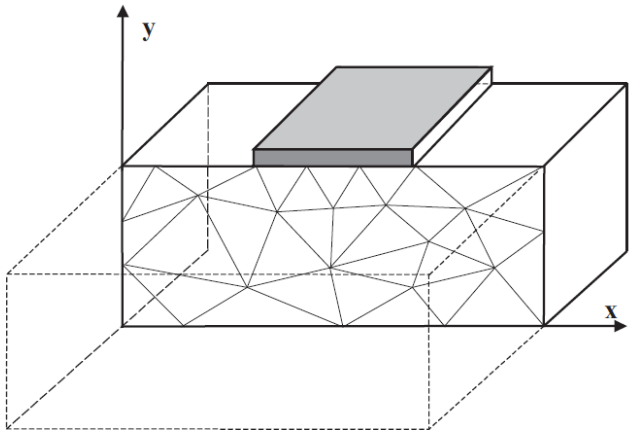


**Figure 2.6:** Visualization of the Plane strain model in Plaxis 2D (Brinkgreve et al., 2011).

### 2.6.2 Modelling piles

Modelling piles may be done using numerical tools such as Plaxis 2D. There are different ways of modelling piles in the Plaxis software such as fixed-end anchors, plates, embedded beam row (EBR) and soil clusters (Brinkgreve et al., 2011). Soil clusters can be used to model piles by giving it the properties of a given structural element. However, as there are great differences in terms of unit weight and stiffness to adjacent soil, errors such as out of balance forces may develop. Another limitation by using soil clusters is that it will be considered as a wall element hence no consideration will be given to movement of soil between piles in the out of plane direction.

When using fixed-end anchor for pile simulation, no consideration of interaction between soil and pile is accounted for. Hence, the use of this alternative should be evaluated as a simplified method, since that interaction occurs in reality (Brinkgreve et al., 2011). When using plates for modelling piles, bending and axial stiffness of the plate are essential material properties. Plates are beam elements with three degrees of freedom per node and the elements are allowed to deflect due to shearing and bending which can be useful when conducting a structural analysis. By using EBR, a pile row can be modelled when using a plane strain model. The obtained displacements when using EBR are the average displacements. When using EBR in Plaxis 2D, the beam elements are defined by 3 nodes if 6-noded soil elements are used or 5 nodes with 15-noded soil elements (Brinkgreve et al., 2011). The implementation of EBR allows the beam to deflect due to shearing and bending but also element changes in terms of length when axial forces are initiated in the model. EBR can therefore be considered as a hybrid of a node to node anchor and a plate.

### 2.6.3 Modelling of impact from pile

As mentioned, the program Plaxis 2D offers several options regarding pile modelling. However, the alternatives are more suitable for cases considering loading problems such as bearing capacity. This is not the same as looking at the installation effects from piling as described in section 2.2. In order to model such behaviour, there are two methods that have not yet been verified but used by many such as Castro and Karstunen (2010), Edstam and Kullingsjö (2011), Dijkstra et al. (2011).

#### 2.6.3.1 Volume expansion

By means of volume expansion, the volumetric strain option is referred to in the program Plaxis 2D. This alternative allows the user to increase the volume of a soil cluster by increasing the strains in the x,z or y-direction or the total volumetric strain. Positive values in the input in terms of strains represents an expansion, and negative ones represents shrinkage. When applied the software ensures equilibrium in the output, between boundary conditions and the affected cluster, by adjusting stresses and forces in the surrounding soil (Brinkgreve et al., 2011). This means that the stiffness in the surrounding soil have a direct effect on the final stresses and deformations. It is therefore of importance to regard the relation between stiffness and the volumetric strain since it can affect the efficiency of the volume expansion of the cluster. Another remark is that the magnitude of strains is strictly related to the soil cluster and not necessarily to the geometry of the model. When the volumetric strain is applied, the magnitude should be calculated with respect to the investigated case and not with respect to the Plaxis model.

#### 2.6.3.2 Prescribed line displacement

Prescribed displacements in Plaxis 2D are special conditions that can be used to control the displacements in certain locations (Brinkgreve et al., 2011). The function can be used on structures, soil clusters or the soil itself. When used, the displacement will occur in the direction and magnitude applied. By adding a prescribed displacement, the soil will displace with the given input in metres. When modelling the impact of piles in undrained conditions, this function can be used on the soil to represent a cavity expansion in axisymmetry (Castro & Karstunen, 2010). This is done by expanding a cavity from a finite initial radius to a final one. To have a finite initial radius is considered to be important, since it cannot start from zero. In comparison with the volumetric strain option this one is considered to be more stable from a numerical simulation point of view (Castro & Karstunen, 2010). In order to reflect the behavior between soil and pile, it is favorable to use interfaces with the prescribed displacement. This in order to catch the interaction, which otherwise is not done since the created cavity is not replaced with a material.

### 2.6.4 Impact from pile group

The group effect from piles will as mentioned in section 2.2 result in larger displacements. In order to reflect the complex behaviour of the impact from a pile group, assumptions (super positioning) must be made. According to Potts, Zdravkovic, and Zdravković (2001) the simple superposition method assumes that the deformations at the ground surface from several piles can be evaluated with a single pile analysis. Thus can the displacements from a pile group be obtained by adding the contribution of displacement from each pile in the group. The impact from each pile is best described with cylindrical coordinates, when the simple superposition technique is applied a transformation to Cartesian coordinates is necessary to describe the displacement vectors for the ”superpile” (Potts et al., 2001). This method is best suitable for prediction of displacements of the ground surface, Potts et al. emphasizes that there are other superposition methods more appropriate for describing the deformations with depth.

# 3
# Methods

## 3.1 Study Area

This thesis focused on a case study involving a construction of 4 low-rise apartment buildings and a car park on Hisingen, Fyrklöversgatan more precisely, a project initiated by Stena Fastigheter. The project involved several construction stages including excavations and piling. Piles was the ground improvement method suggested from the conducted geotechnical investigation and a total of 1186 piles with different dimensions were installed in the area. The study was based on the information and the parameters interpreted from the geotechnical investigation in the area. The measurements performed in order to detect the displacements of the soil were the benchmark for this thesis. In order to achieve comparable results with field measurements, the study focused on modelling a pile row in the area of the car park (block E), which is circled as can be seen in figure 3.1. This since it was found that modelling the last pile row (M1) to the south of the car park was the closest to the measurement points 1,2 and 3 (see appendix A). The measurement points have been placed outside the construction area in order to observe the surrounding effects from piling activities and other construction related activities. Those are marked with different numbers and are illustrated in figure 3.1.

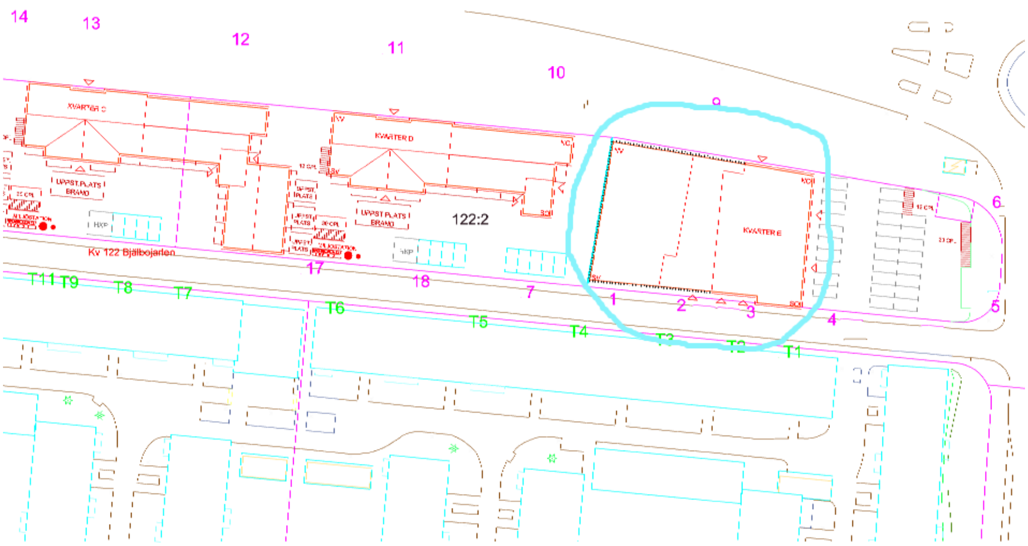


**Figure 3.1:** A section of the study area where block E is circled and the measurement points are pointed out.

## 3.2 Soil profile and properties

The geotechnical properties of the soil in the area were provided from tests conducted on two boreholes, NC2 and NC7 west of block E (see figure 3.2). The gathered information from the boreholes are assumed to be representative for the whole stretch including the investigated car park.

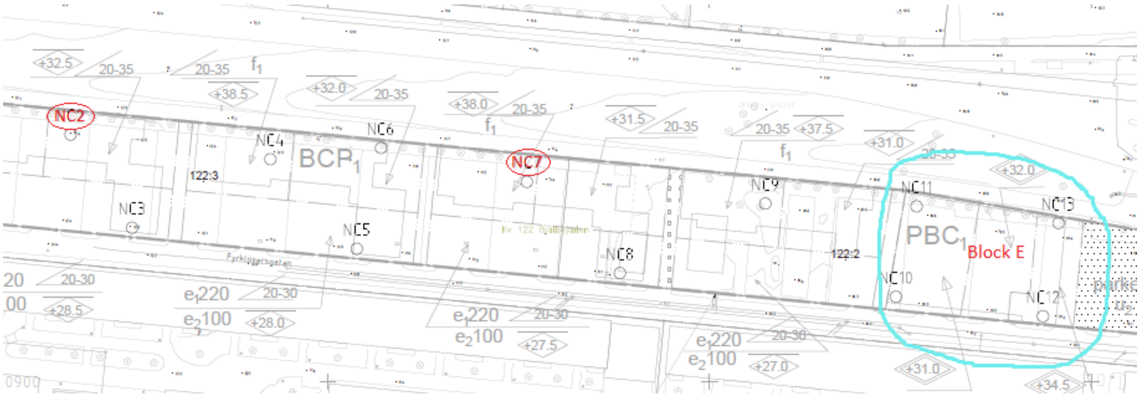


**Figure 3.2:** Location of the two boreholes NC2 and NC7.

Different tests were conducted in order to achieve relevant properties for the soil of the project. As seen in table 3.1, different tests were performed depending on the environment either in laboratory or on site, to attain useful information. The cone penetration test (CPT) was only performed in borehole NC2. The predicted displacement of soil due to the presence of piles required parameters that were derived from the performed investigation and the use of empirical relations. The soil profile was determined from the performed tests on the soil, both on site and in the laboratory, with consideration given to the liquid limit, sensitivity, permeability, OCR, density of soil and undrained shear strength (see Appendix B). The soil profile was divided into 4 layers where of 3 layers consists of clay and a top layer of fill.

**Table 3.1:** Different types of tests conducted on the two boreholes NC2 and NC7.

| **On site** | **Laboratory** |
|---|---|
| CPT | Direct shear test |
| Soil/Rock probing | Cone sample |
| Pyramid penetration test | Liquid limit |
| Vane test | Water content |
| Sample test | Bulk density |
| Ground water measure | CRS |
| Pore pressure test | Classification |

Constant Rate of Strain (CRS) test were conducted at 8-, 12-, 20-, 30-, 40- and 50-meters of depth in borehole NC2 and at 30-, 40- and 50- meters in borehole NC7. From the CRS tests performed on several depths the preconsolidation pressure ($\sigma'_c$) was obtained. These interpretations displayed that the soil exhibited characteristics of slightly over consolidated clay (see table 3.2). From the tests performed it could be stated that clay was dominant throughout the soil profile. From the CPT and laboratory tests, the magnitude of the fill was estimated to 1,5 meters. The magnitude of the clay layer in the area was estimated to 50 meters. In point 10 at a depth of 48 meters, the probe hit material that could not be driven further by using a conventional method. Below the clay, measurements indicated that a layer with higher strength is present. The parameters for the soil layers were derived by interpretation of the results from the same tests that were used for the soil profile (see Appendix B). No triaxial tests were performed for the project of scope in this thesis.

**Table 3.2:** Interpreted OCR values for different depths.

| **Depth** | 1.5-12 metres | 12-40 metres | 40-50 metres |
|---|---|---|---|
| **OCR** | 1.08 | 1.4 | 1.27 |

The evaluated OCR indicated that OCR varied with depth. However, as no CRS were performed for soil from 1,5 to 8 meters of depth, assumptions were made. $\sigma'_c$ was calculated empirically using Hansbo's formula in order to describe the preconsolidation for the soil above 8 meters of depth. The obtained preconsolidation pressures using Hansbo's formula were discarded. However, as the soil properties for the overlaying soil (1,5 to 8m of depth) were evaluated (see Appendix B) , it was assumed that the clay in this section was the same from 1,5 meters to 12 meters of depth. The interpretation of the preconsolidation pressures for the overlaying layers were thereby not made directly. However by interpolating OCR with respect to CPT and the standard routine tests performed in laboratory, it was possible to calculate $\sigma'_c$, as the total vertical effective stress was determined by using Terzaghi's principle (see figure B.2 in Appendix B).

**Table 3.3:** Pore pressures obtained from CPT.

| Depth [m] | Pressure [kPa] |
|---|---|
| -1,5 | 0 |
| -40 | 395 |

The CPT indicated that the pore pressure at 40 meters of depth was 395 kPa (see table 3.3). With the ground water table at 1,5 meters of depth, the gradient of the pore pressure was 10,3 kPa/m. For simplicity, the pore pressures were assumed as hydrostatic (i.e. 10 kPa/m) as the difference of 0,3kPa meters was considered as negligible.

The values for $\kappa^*$ and $\lambda^*$ were derived by interpreting the performed CRS-tests as illustrated in figure 3.3 (M. Olsson, 2010). The interpreted values for A and B were used in equation 3.1 and 3.2 in order to estimate values for $\kappa^*$ and $\lambda^*$.

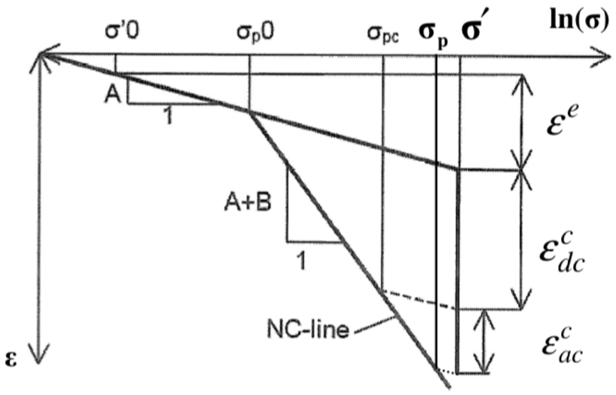


**Figure 3.3:** Idealized and modified stress-strain curve (M. Olsson, 2010).

$$\kappa^* \approx \frac{3 \cdot (1 - v_{ur})}{(1 + v_{ur}}) \cdot A \tag{3.1}$$

$$\lambda^* = B + \kappa^* \tag{3.2}$$

The obtained values when using the method illustrated in figure 3.3 and by calculating $\kappa^*$ & $\lambda^*$ using equation 3.1 and equation 3.2 are presented in figure 3.4

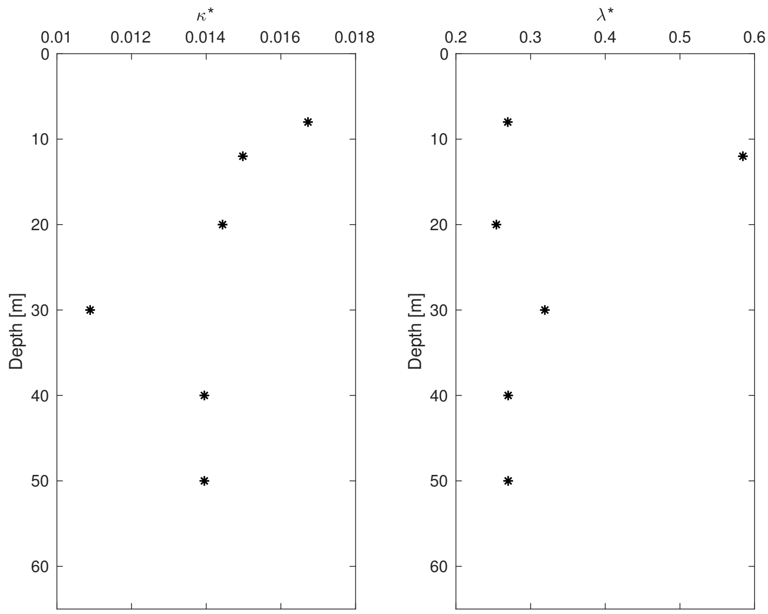


**Figure 3.4:** Obtained values for $\kappa*$ and $\lambda^*$ from CRS for different depths.

## 3.3 Conceptual model

With the data from the performed geotechnical investigation and the geometry of the study case, a conceptual model was created (see figure 3.5). The length of the investigated rectangular piles was 46 metres with a width of 0,24 metres. The piles were driven 1,5 meters below surface level, since these were among the first piles driven in the area before the excavation was carried out. No sheet pile wall was installed in this early stage, only a 1:3 excavation, and therefore no sheet pile wall was included in the analysis.

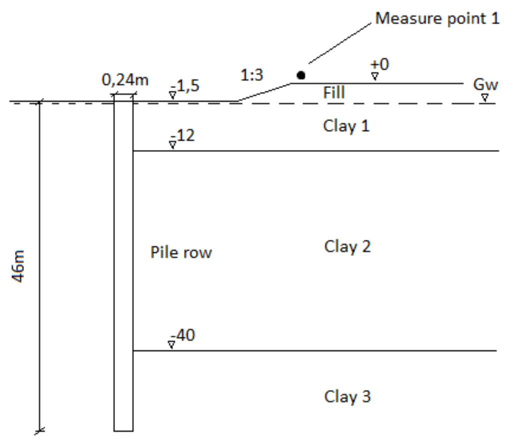


**Figure 3.5:** A conceptual model of the modelled pile row seen in section (not made to scale).

In order to conduct a reasonable analysis of the deformations from the pile row, some limitations were set. The available measurements from field was limited to show the displacement day wise. In order to compare the modelled results with field measurements, the modelled piles were all installed on the same day. They were also the only ones installed close to measure point 1, this was found important in order to reduce the risk of the results being influenced by other piles. Seven piles from the previous mentioned pile row M1 were chosen accordingly, see figure 3.6 for more information regarding the geometry. In figure 3.6 the piles are circular, this since an effective radius was created for later calculation stages (see Appendix A).

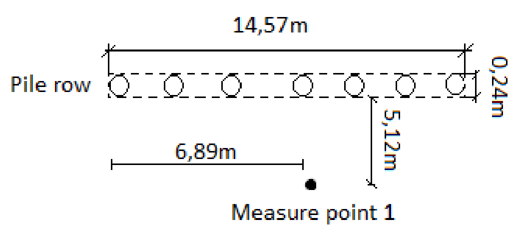


**Figure 3.6:** A conceptual model of the modelled pile row seen from above (not made to scale).

## 3.4 Numerical modelling using Plaxis 2D

The modelling of the case study was carried out using finite element software Plaxis 2D for the numerical estimation and SSPM for the analytic estimation of the displacements.

For the analysis conducted in Plaxis 2D, some assumptions and model setups for the given project were made. The project properties for the model were set up using plane strain assumption since it was best suitable for modelling a pile row and 15-noded soil elements were chosen. The size of the model was set to be 3 times the depth of soil, resulting in 150 meters in both directions making the model 300 meters long stretching from -150 to 150 meters. No elevation of the soil profile was implemented in order to simplify the model. The groundwater table was set at 1,5 meters of depth from ground surface assuming hydrostatic conditions as described in section 3.2.

### 3.4.1 Model setup

The input parameters used for the model set up are presented in table 3.4. The soil layers in the model set up used in Plaxis 2D were set accordingly as described in section 3.2.

**Table 3.4:** Properties for the layers in Plaxis 2D.

| **Description** | **Symbol/Name** | **Unit** | **Fill** | **Clay 1** | **Clay 2** | **Clay 3** |
|---|---|---|---|---|---|---|
| Depth | $z$ | [m] | 0-1.5 | 1.5-12 | 12-40 | 40-65 |
| ***General*** | | | | | | |
| Material model | *Model* | - | Linear elastic | Soft Soil | Soft Soil | Soft Soil |
| Drainage type | *Type* | - | Drained | Undrained (A) | Undrained (A) | Undrained (A) |
| Dry weight | $\gamma_{unsat}$ | $[kN/m^3]$ | 18 | 15 | 16.3 | 18 |
| Wet weight | $\gamma_{sat}$ | $[kN/m^3]$ | 20 | 15 | 16.3 | 18 |
| ***Parameters*** | | | | | | |
| Modified Compression index | $\lambda^*$ | - | - | 0.22 | 0.23 | 0.20 |
| Modified swelling index | $\kappa^*$ | - | - | 0.012 | 0.008 | 0.010 |
| Young's modulus | $E'$ | [Mpa] | 10 | - | - | - |
| Effective Poisson's ratio | $\nu'$ | - | 0.35 | - | - | - |
| Poisson's ratio unloading-reloading | $\nu_{ur}$ | - | - | 0.15 | 0.15 | 0.15 |
| Cohesion | $c'$ | [kPa] | 0 | 1.6 | 4.5 | 7.5 |
| Friction angle | $\phi'$ | [°] | 0 | 30 | 30 | 30 |
| Dilatancy angle | $\Psi$ | [°] | 0 | 0 | 0 | 0 |
| ***Ground water*** | | | | | | |
| Permeability in horizontal direction | $k_x$ | [m/day] | $1 * 10^-3$ | $0.095 * 10^-3$ | $0.04 * 10^-3$ | $0.025 * 10^-3$ |
| Permeability in vertical direction | $k_y$ | [m/day] | $1 * 10^-3$ | $0.095 * 10^-3$ | $0.04 * 10^-3$ | $0.025 * 10^-3$ |
| ***Interfaces*** | | | | | | |
| Interface strength | - | - | Rigid | Rigid | Rigid | Rigid |
| Interface reduction strength | $R_{inter}$ | - | 1 | 1 | 1 | 1 |
| ***Initial*** | | | | | | |
| $K_0$ determintation | - | - | Automatic | Automatic | Automatic | Automatic |
| Lateral earth pressure coefficient | $K_{0x}$ | - | 1 | 0.5324 | 0.6294 | 0.5809 |
| Over-consolidation ratio | $OCR$ | - | - | 1.08 | 1.4 | 1.27 |

The **general set up** in the model can be seen in table 3.4. The material model used for the clay layers was the SS-model and the LE-model was used to model the behaviour of the fill material. The SS-model was chosen for the clay as the clay exhibits light overconsolidated characteristics (see table 3.2). Deformations were the scope of the analysis and additionally, the SS-model is able to account for non-linear stiffness thus using the SS-model for a deformation analysis is suitable as presented by (Karstunen et al., 2017). It was also found that due to the available data and conducted tests in the area of scope, parameters necessary for modelling using the SS-model could be derived which was beneficial instead of using empirical values for key parameters if another material model was used.

The **drainage type** was set as Undrained (A) for the clay layers in order to enable an effective stress analysis. Due to the low permeability of the clay and by conducting an undrained analysis, the dry and wet unit weight of the clay was set as equal. For the fill layer, the drained option was used as drainage type as its permeability is significantly higher than the underlying clay layers.

Derived material properties were calibrated towards results from the soil test function using CRS. -16,8%/day was used in soil test as this was the pace that the test provided by Norconsult AB was carried out in. The optimization of the parameters were later done in excel by changing the key parameters used for the soft soil model that affects the output from a specific CRS-test. This was made in order to assure that the model predicts the behaviour of the soil as in reality as good as possible. As stated earlier, the clay on site is divided in to three layers. The second layer stretched from 12 to 40 meters of depth and CRS-tests were performed on 20, 30 and 40 meters of depth. During the calibration of the parameters, the values that were optimized for one depth within the layer, were later applied to another test in the same layer. This was made in order to obtain reasonable and representative values for the required parameters in the detected layers. The parameters that were calibrated are presented in section ***parameters*** in table 3.4. Calibration using the "Soil test" tool with the SS-model in Plaxis 2D for CRS at a depth of 40 meters is presented in figure 3.7.

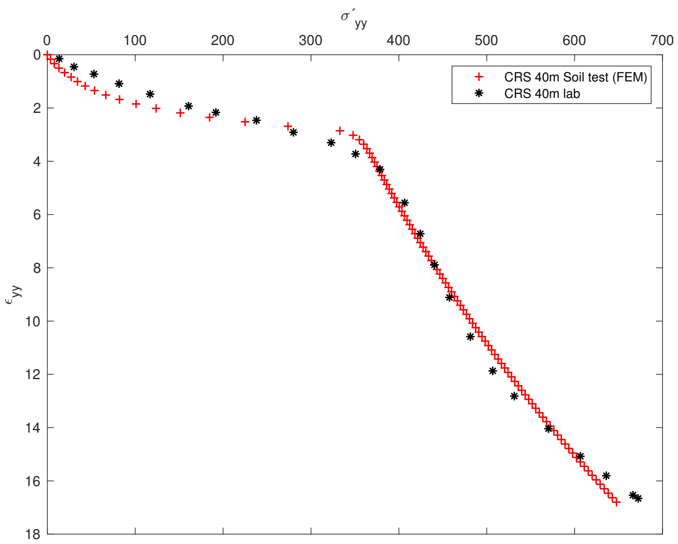


**Figure 3.7:** CRS from Soil test vs CRS from lab at 40 meters of depth (Borehole NC7).

For calibration of remaining depths, see Appendix C.

In order to validate that the calibration of the parameters using Soil test in Plaxis 2D were representative. The constant constrained modulus below the effective vertical preconsolidation pressure ($M_0$) was evaluated for several depths (see table 3.5). According to (M. Olsson, 2010), the interpreted value for $M_0$ from CRS tests should be multiplied by a factor 3 to 5 in order to verify that the behaviour is similar to the actual behaviour of soil. The obtained values from Soil test in Plaxis 2D were approximately 3 times the value given by CRS tests (see table 3.5).

**Table 3.5:** Table of modulus values used to validate the calibration.

| **Depth** | $M_{0P}$ **[Pa] Plaxis** | $M_{0C}$ **[Pa] CRS** | $M_{0P}/M_{0C}$ |
|---|---|---|---|
| 8 | $3.98 \cdot 10^6$ | $1.6 \cdot 10^6$ | 2,49 |
| 12 | $10.5 \cdot 10^6$ | $3.6 \cdot 10^6$ | 2,92 |
| 20 | $19.1 \cdot 10^6$ | $6.6 \cdot 10^6$ | 2,89 |
| 30 | $21.6 \cdot 10^6$ | $7.4 \cdot 10^6$ | 2,92 |
| 40 | $32.1 \cdot 10^6$ | $10.5 \cdot 10^6$ | 3,06 |
| 50 | $32.4 \cdot 10^6$ | $11.0 \cdot 10^6$ | 2,95 |

The friction angle at critical state was assumed to be 30°. The cohesion intercept (c') was calculated for each layer using equation 3.3.

$$c' = 0,1 \cdot c_u \tag{3.3}$$

Poisson's ratio for unloading-reloading $v_{ur}$, was set to 0,15 due to the soil being considered as soft. Accordingly Karstunen et al. (2017) states that $0,1 < \nu_{ur} < 0,2$ for soft soils. The dilatancy angle ($\psi$) was set to 0 due to the SS-model's application of Mohr Coulomb failure condition, hence no plastic volumetric strain at failure is obtained (Karstunen et al., 2017).

The permeability of the soil layers were interpreted from CRS-tests. As seen in table 3.4, the permeability was assumed equal in both horizontal and vertical direction due to no consideration given to anisotropy of soil. The permeability for the fill material was assumed to be approximately 10 times greater than the permeability of the underlying clay layer.

### 3.4.2 Calculation method

The model initiated in Plaxis 2D can be seen in figure 3.8, this is a section of the beginning of the pile row, where Measure point 1 is located to the right of the y-axis. The boundary conditions were set to normally fixed horizontally, totally fixed at the bottom and free at the ground surface. The model was considered large enough in order to obtain satisfactory behavior of the soil. For the ground water, all boundaries except the bottom ($Y_{min}$) was set to free. By refining the mesh locally and using the fine option for element distribution, a satisfactory mesh was created. The same plaxis-model was used for modelling the impact from piles with the two methods: volume expansion and line displacement, see Appendix D for figures of the two scenarios. The slight difference of modelling with line displacement was that a symmetry line was created in the middle of the pile. Thus, not affecting the outcome due to symmetry, resulting in a closed boundary condition for the ground water at $X_{min}$.

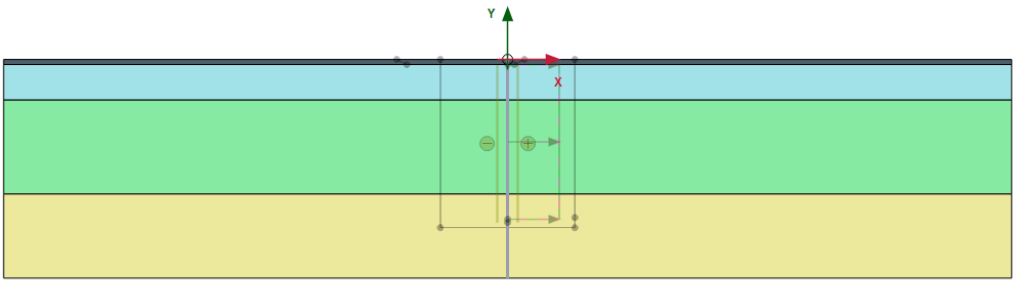


**Figure 3.8:** Model initiated in Plaxis 2D.

The volume expansion and line displacement were calculated by considering that the existing volume of soil in the analyzed pile area would increase with the volume of driven piles, as described for the undrained case in section 2.2. This resulted in a calculation were the difference of the volume of the piling area with and without the driven piles (see Appendix E). The volume of the seven piles that were driven on the same day were added to the volume of the piling area which can be considered as a rectangular wall of soil, matching the geometric properties of the pile row presented in figures 3.5 and 3.6.

The magnitude of the line displacement in Plaxis were calculated by using the following equation:

$$Prescribed - line - displacement = (r_2 - r_1)/2 \tag{3.4}$$

Where:
$r_2$ = New width/radius of piling area
$r_1$ = Width/radius of piling area.

The line displacement function was considered representative, since it will displace the added volume from each pile as proposed in section 2.6.4. Equation 3.4 accounts for the displacement of soil in one direction, and this direction is towards measure point 1 in the Plaxis model. Equation 3.4 can be used if half of the investigated area is modelled with a symmetry line as seen in Appendix D in figure D.2.

For the volume expansion, a soil cluster corresponding to the pile area was created which later on was expanded with a certain percentage. The expansion in percentage was calculated with the following equation:

$$\varepsilon_{vx} = (r_2 - r_1)/r_1 \tag{3.5}$$

Where:
$r_2$ = New width/radius of piling area
$r_1$ = Width/radius of piling area.
$\varepsilon_{vx}$ = Volumetric strain in the x-direction.

This method is also considered representative in plane strain since the theoretical pile area of soil was modelled as a soil cluster. The added volume from the pile driving was expressed in terms of an expansion of strains in the x-direction. The same mindset, as for the line displacement, regarding superpositioning by conservation of volume was implemented.

With the model setup and the calculations made, the last step was to set up the different phases in Plaxis. The different phases in the staged construction menu is presented in table 3.6.

**Table 3.6:** Table of the different phases in Plaxis 2D.

| **Phase** | **Type** | **Event** |
|---|---|---|
| Initial | K0 procedure | Creating initial stresses |
| Phase 1 | Plastic | Excavation of first 1,5m |
| Phase 2 | Plastic | Activation of Line displacement /Volumetric strain |
| Phase 3 | Consolidation | Until minimum excess pore pressure |

The phase setup was the same for the two different models initiated with the two different methods for pile driving. This means that phase 2 could only activate either the line displacement or the volumetric strain since they were not modelled in the same model. The consolidation phase is an added phase in order to confirm that the model is numerically stable enough to perform a consolidation analysis.

## 3.5 Analytic calculation

The analytic solution was performed by using SSPM. This was made in order to compare the results from the numerical solution made in Plaxis 2D with the obtained results by using SSPM. SSPM was implemented by investigating the displacements at the ground surface, $z = 0$, thus equation 2.8 and 2.7 was used. The calculation was carried out in R-studio by using code for expressing the equations. The results from R-studio could later be plotted with different computer tools. When using SSPM for the simple pile solution, super-positioning was implemented in order to achieve the total displacements from the pile group. However, as a pile row in plane strain was modelled in Plaxis, the case of simple wall was also calculated by using equation 2.6 and 2.5 (see Appendix E). By using the equations for simple wall given in SSPM-theory, the piles are assumed to behave like a retaining wall considering displacements. This behaviour was later compared with the numerical methods calculated in Plaxis 2D. For simple pile, 80 meters of distance from the pile was considered whilst for the simple wall 150 meters was considered.

## 3.6 Sensitivity analysis

A sensitivity analysis regarding the horizontal and vertical displacements obtained by the numerical calculation was conducted. This was made by investigating the parameters used when modelling with the SS-model. The parameters that were evaluated are $\kappa^*$, $\lambda^*$, $\nu_{ur}$, $\phi'$ and $c'$. The sensitivity analysis was made in order to create a deeper understanding for which parameters that would influence the displacements the most.

The analysis was conducted by using the "Sensitivity and parameter variation"-tool in Plaxis 2D. The range used for the analysis was set with respect to different interpretations of the given data for the conditions on site. The friction angle was set with a range of $30 - 32°$ and $\nu_{ur}$ was set to vary between 0.1 to 0.2 as suggested by (Karstunen et al., 2017). $c'$ was set to vary in between the range of the interpreted values for $c_u$ obtained from laboratory tests (see figure B.4 in Appendix B). Regarding $\kappa^*$ and $\lambda^*$, the range of uncertainty was set according to the calibration that was performed using SoilTest in Plaxis 2D.

By choosing the parameters of interest and selecting the given range of uncertainty for each, the sensitivity and parameter variation tool offers to look at several options by adding a criterion. In the performed analysis, the criterion to look at the effect different parameters will have on the displacements was chosen. The tool also distinguishes between total displacements or the displacements in the x or y-direction.

There is also a possibility to look at a specific node where the criterion will be applied. In this analysis the node where measure point 1 is found, was chosen.

# 4
# Results

The results obtained for this study are presented in this chapter. The displacements from each prediction method have been normalized with the diameter of the pile, in order to make the methods comparable with each other. The results will be presented in a graphs, tables and later compared with each other before the sensitivity analysis. When comparing the results, interpolation of the deformations obtained from SSPM simple pile solution was made with respect to a distance of 150 metres. The presented deformations are present at the ground surface only.

## 4.1 Results from Plaxis

The results obtained from Plaxis using the volume expansion and line displacement functions can be seen in figures 4.1 and 4.2. The calculated displacements plotted over a stretch, corresponding to the width of the model from source, gives the curves. Those shows the behaviour of the soil by illustrating the displacement at a certain distance. For the displacements in the horizontal direction ($u_x$) in figure 4.1, it can be seen that the displacements are zero at a distance of 150 metres. For the vertical displacements ($u_y$) the results indicates that the displacements has not yet decreased to zero in the range of the modelled length of the initiated model.

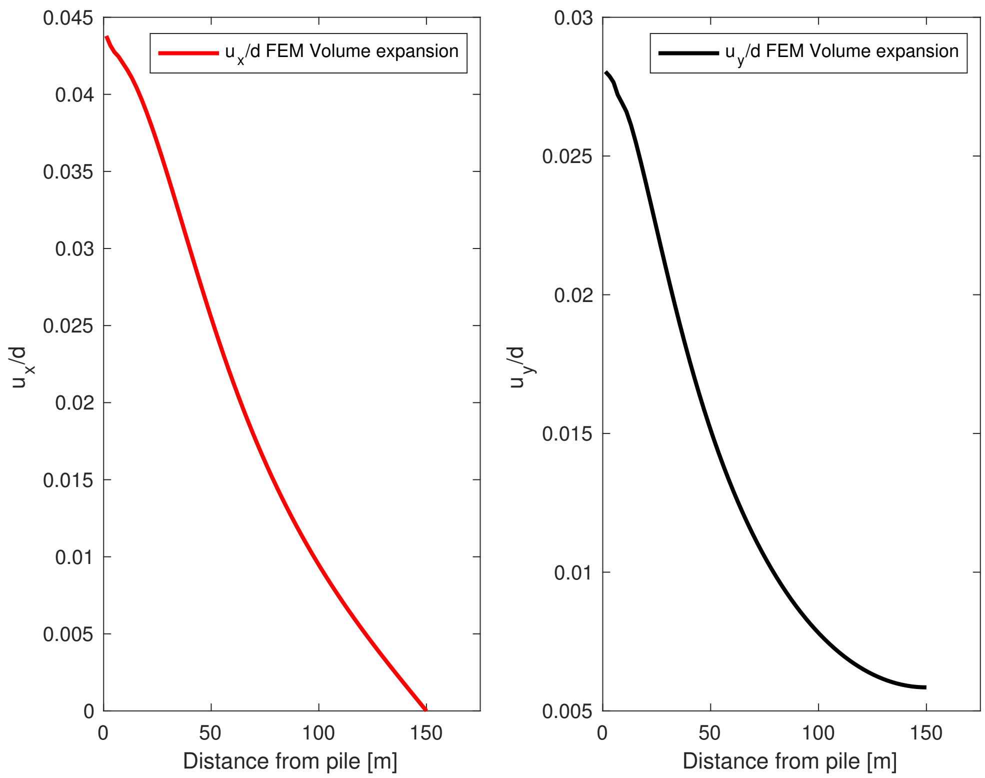


**Figure 4.1:** Deformations using volume expansion in Plaxis 2D.

The graphs in figure 4.2 representing the obtained displacements when using the line displacement function, corresponds well to the obtained displacement when using the volumetric expansion method. The horizontal displacement decreases and reaches a value of zero 150 metres from the pile penetration point. For the vertical displacement, it can be seen that the deformations on the ground surface has not subsided completely at a distance of 150 meter.

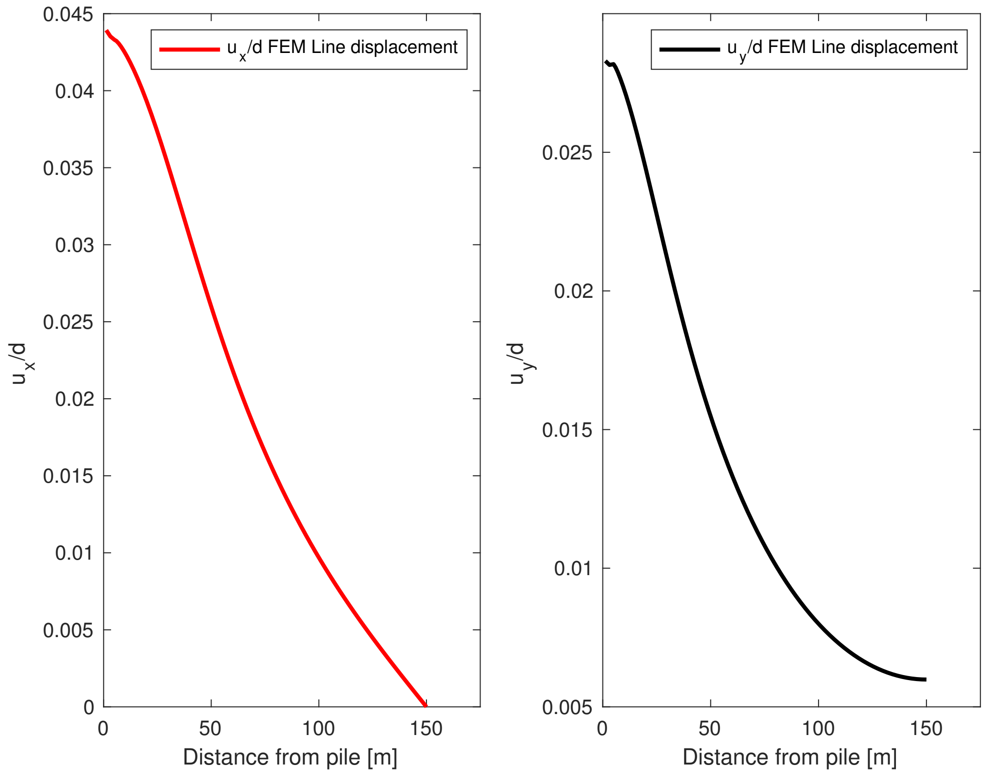


**Figure 4.2:** Deformations using Line displacement in Plaxis 2D.

The behaviour of the curves in figure 4.1 and 4.2 are also similar. This indicates that the results from the numerical analysis using Plaxis 2D with the current model set up, are similar when using the two different methods.

Another remark is that the peak values obtained close to the pile is approximately of the same magnitude for the displacements in both directions analyzed, in the two figures 4.1 and 4.2.

## 4.2 Results SSPM

In comparison to the deformations in section 4.1, the obtained deformations using SSPM with simple wall and simple pile solution decreases more initially (see figure 4.3 and 4.4). The obtained horizontal deformations using the simple wall solution for SSPM does not converge to zero at a distance of 150 meters. Considering the vertical displacement, the graph in figure 4.3 indicates that they converges to zero as the distance from the pile increases. However, the vertical displacements nor the horizontal displacements are zero at 150 meters from the pile penetration point as illustrated in figure 4.3.

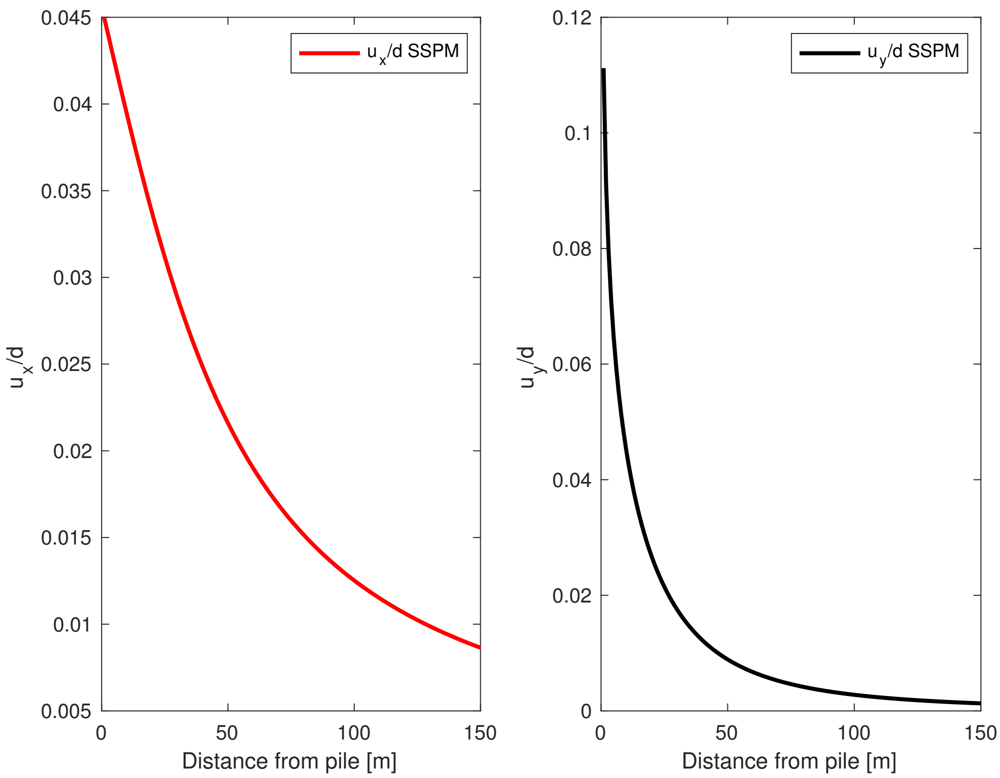


**Figure 4.3:** Deformations using SSPM with simple wall.

The results obtained from SSPM with the simple pile solution displays different horizontal displacement (see figure 4.4) than the simple wall solution. The behaviour for the displacements in the both directions using the simple pile solution is very similar. However, the magnitude of the deformations is not similar as the horizontal displacements are larger than the vertical displacements close to the pile and at 80 meters of distance from the pile. At 80 meters from the pile, the vertical displacements converges to zero while the horizontal displacements has not converged to zero at the considered distance of 80 meters as illustrated in figure 4.4.

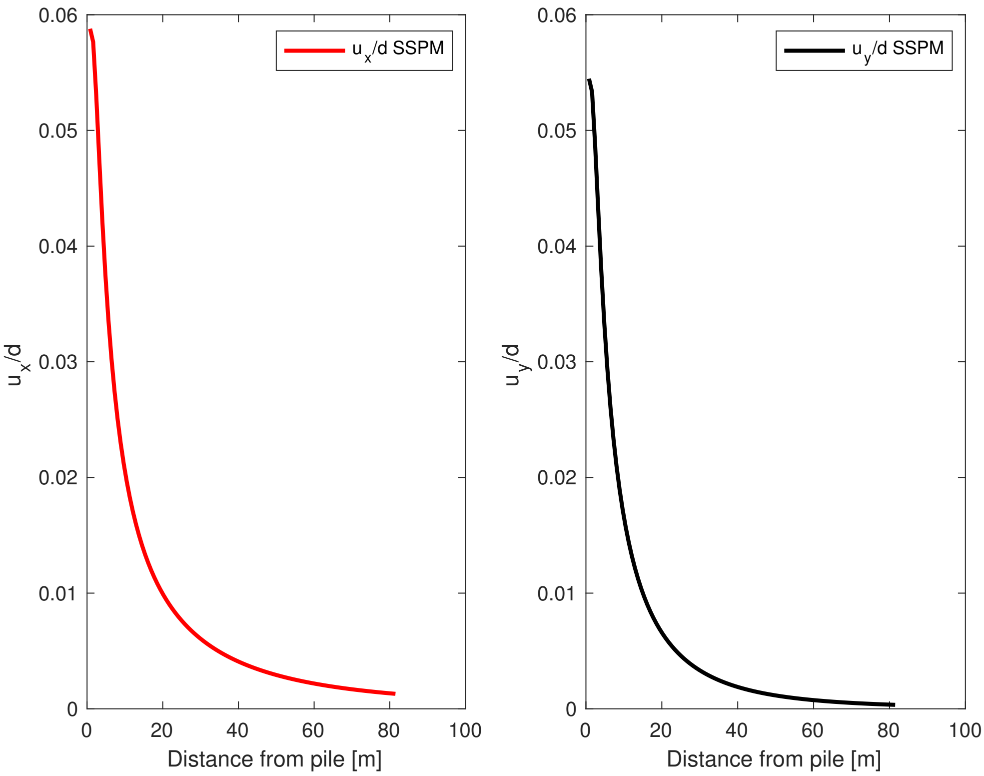


**Figure 4.4:** Deformations using SSPM with simple pile.

The results obtained from simple wall and simple pile solutions deviates from each other, in comparison to the results obtained from the numerical analysis in section 4.1. The obtained magnitude of the deformations is different for the two methods, see figure 4.3 and 4.4. However, the behaviour of the decrease of the deformations is similar. It should be noted that the deformations obtained using the simple pile solution (see figure 4.4) flatter out earlier than the curves for the simple wall solution in figure 4.3. Also, the curve showing the horizontal displacements for the simple wall solution in figure 4.3 deviate from the other curves obtained, by using the different methods categorized as SSPM methods.

## 4.3 Field measurement

In table 4.1 the obtained displacements from the different prediction methods and field measurements are presented. The values are presented in millimeters and not in normalized values as in the graphs. This in order to make the deformations comparable with the data from measure point 1.

**Table 4.1:** Predicted and measured displacements.

| Method | Horizontal Displacement | Vertical Displacement |
|---|---|---|
| SSPM Simple pile | 8,92 mm | 7,91 mm |
| SSPM Simple Wall | 10,23 mm | 15,51 mm |
| PLAXIS Volume Expansion | 10,26 mm | 6,64 mm |
| PLAXIS Line Displacement | 10,39 mm | 6,76 mm |
| **Measure point 1** | **9,58 mm** | **8,72 mm** |

The values are in the same range, except for the vertical displacement obtained using the SSPM simple wall solution. However, to truly reflect the deviation for such small deformations a comparison in percentage is most suitable. Table 4.2 below shows the differential between the different prediction methods and the obtained measurements from field in percent. Overestimated displacements are noted with a + and underestimated displacements are noted with a - (see table 4.2).

**Table 4.2:** Deviation using the scoped models against field measurements in percent.

| Method | Horizontal Displacement Deviation | Vertical Displacement Deviation |
|---|---|---|
| SSPM Simple pile | -6,89 % | -9,29% |
| SSPM Simple Wall | +6,78 % | +77,87% |
| PLAXIS Volume Expansion | +7,09 % | -23,85% |
| PLAXIS Line Displacement | +8,46 % | -23,48% |

## 4.4 Comparison

By plotting all the curves for the deformations in one graph (see figure 4.5), differences between the different prediction methods becomes more distinct. In figure 4.5 it can be observed that the numerical modelling with the two methods used, resulted in almost identical behaviour. This outcome of the numerical analysis can also be observed when evaluating the vertical displacements seen in figure 4.6. Therefore, the methods used in numerical analysis will be compared with the rest as one. Regarding the behaviour of curves looking at horizontal displacements, the simple wall solution and Plaxis methods suits best of the three. The SSPM simple pile solution deviates from the results obtained from the numerical analysis and the simple wall solution (see figure 4.5). This curve has also the highest peak value when considering displacements close to the pile. According to section 4.3, all the prediction methods deviates less than 10% compared to the measurements from field. But in figure 4.5 it is shown that the simple pile solution would have differed the most if measure point 1 would have been located closer. While the simple wall and the Plaxis methods would indicate values close to each other.

Figure 4.5 show that the SSPM simple wall solution is not decreasing enough to converge to zero within 150 metres. While the other two prediction curves shows that they are decreasing enough in order for the displacements to finally cease.

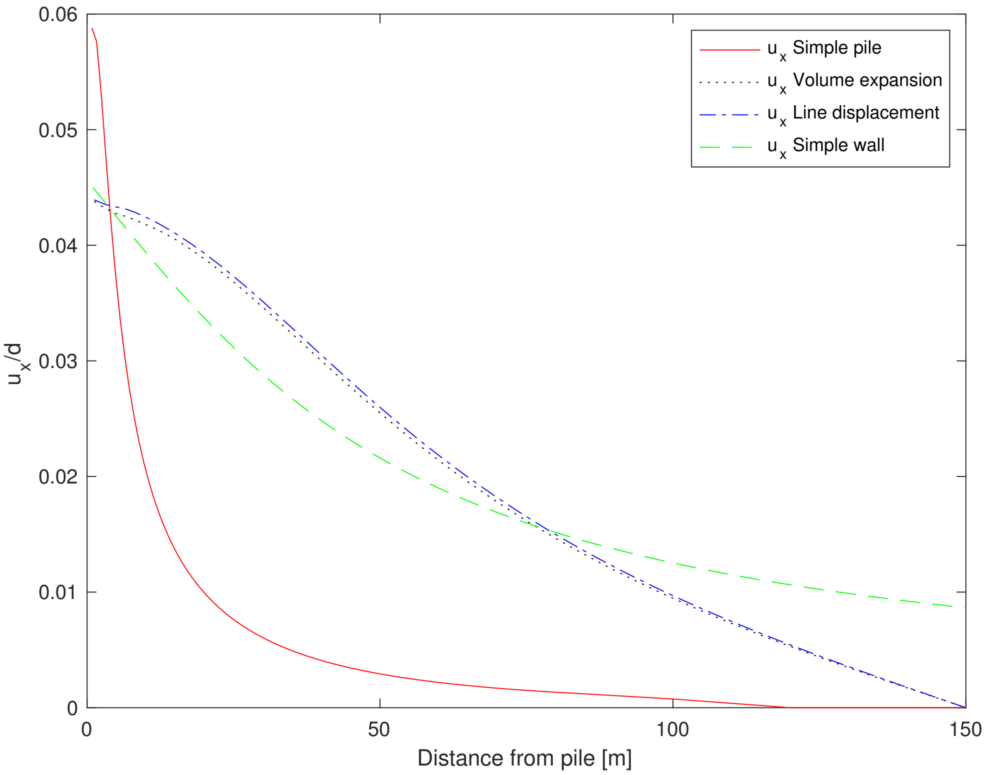


**Figure 4.5:** Normalized horizontal displacements.

When regarding the vertical displacement (see figure 4.6), the behaviour of the displacements over distance from the pile is different than for the horizontal displacements. In this case the SSPM methods seems to suit best of the three regarding the behaviour, despite the big difference in magnitude. The initial vertical displacement from the simple wall solution deviates compared with the other methods.
The Plaxis methods decreases but does not converge to zero at a distance of 150 metres. However, the prediction method matching the measured vertical displacement the best is the SSPM simple pile solution. Comparing the other curves with the one for simple pile, it is observed that the range of difference is large. Again the simple pile curve is giving high values of displacement close to the pile, the simple wall solution indicates the same thing. The Plaxis methods gives a low peak value compared with the other curves.

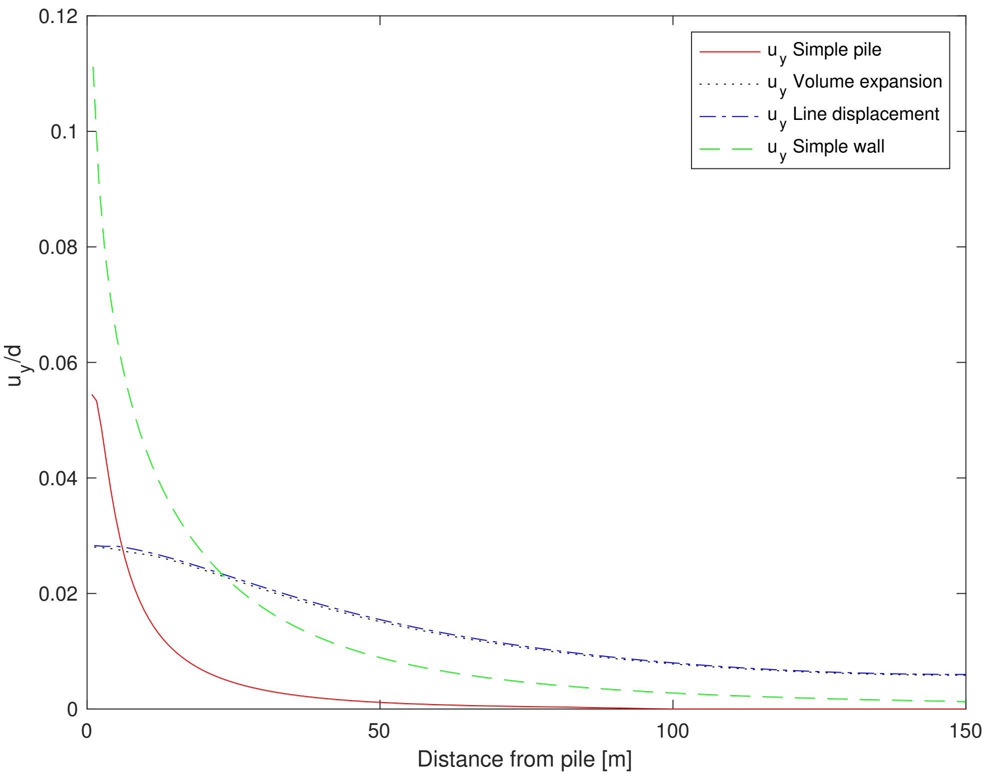


**Figure 4.6:** Normalized vertical displacements.

## 4.5 Sensitivity analysis of input parameters in Plaxis 2D

By using the sensitivity analysis tool in Plaxis 2D the parameters that affects the displacements the most, in comparison with the other evaluated parameters, was given the highest sensitivity score (SensiScore). The specific SensiScores obtained for each clay layer and for the displacements, in each direction, for the two prediction methods can be found in Appendix F and G.

For the model in which the Line displacement method where initiated, the parameters $\nu_{ur}$ and $\kappa^*$ received the highest SensiScores. The observed results of affecting parameters was the same for the displacements both in the vertical and horizontal direction (see Appendix F). An observation was made regarding the variation in SensiScores for the different Clay layers. Close to the surface where Clay 1 is dominating, the influence of $\kappa^*$ is greatest. In Clay 2 the influence of $\nu_{ur}$ exceeds $\kappa^*$, and in Clay 3 the influence of both becomes stable and equal.

The SensiScores for the model where the Volume expansion method was applied, were different. There was a greater variance of affecting parameters for each clay layer (see Appendix G). The $\nu_{ur}$ still had a great influence in each clay layer for displacements in both directions. But there was also an influence of both $\kappa^*$ and $\lambda^*$. One scenario occurred in clay 1 when regarding the vertical displacement where $c'$ had the most influence on the displacements see figure G.4.

# 5
# Discussion

The deformations obtained from the SSPM solutions deviates compared to field measurements. This can depend on that the analytical solutions is based on being applied on the ground surface. As mentioned in section 2.2, the deformations is likely to go from a higher elevation to a lower one. By having an excavation, the magnitude of deformations are likely affected.

The deviation of results from the SSPM simple wall solution may depend on, that a pile row is permeable in reality and will therefore not push all the soil in one direction. The surrounding effects from piles tend to move soil in many directions from pile center. This will lead to an interference of deformations between piles resulting in a lower magnitude of displacements. The center to center distance of piles will therefore be of importance if a pile row is to be considered as a wall.

The performed numerical analysis in Plaxis 2D is accounting for the difference in level, between the ground surface and the position of pile, but is still underestimating the vertical deformations with 24% in both cases. For the horizontal displacements, the analysis overestimates in comparison to the measured data with 7,09 % using Volume Expansion and 8,46 % using Line Displacement (see table 4.2). Beyond numerical and modelling errors the difference in values can be strictly related to the chosen material model. As observed in section 4.5, $\kappa^*$, $\lambda^*$ and $\nu_{ur}$ were the most affecting parameters regarding displacements when using the tool in Plaxis 2D. It would thereby be of interest to perform the analysis with a material model that accounts for small strain stiffness as the model in this thesis overestimates the displacements at the end of the model as it overestimates the strains. However, it should be noted that in order to make such a statement more cases should be evaluated and the evaluation of the input parameters should be correct.

According to Wersäll and Massarsch (2013), the maximum heave occurs in the range between 0.3 to 1 times the pile length. In the case of this thesis, this would be between 13,8 meters to 46 meters from the pile. As seen in figure 4.6, the maximum heave occurs closer to the pile for both numerical methods than suggested by Wersäll and Massarsch (2013). Wersäll and Massarsch states that when superspositioning is applied, it is of importance that the assesed displacements are at a sufficient distance. There is no telling if measurepoint 1 where placed at such a distance. Other reasons might be modelling errors related to material properties such as stiffness used in the soft soil model but also the method used for modelling the installation effect from the piles.

## 5.1 Sources of error

It was also clear that the preconsolidation pressure in terms of OCR is a parameter of importance. As seen in figure B.2, the evaluation of OCR was strictly made by dividing the soil profile in to three layers with constant OCR in each layer. As seen in figure B.2, the strict division of the layers creates a clear deviation from the empirical calculation of OCR by using Hansbo's method to calculate $\sigma'_c$. There is also a clear deviation between 12 and 40 meters of depth from the OCR when using $\sigma'_c$ obtained from CRS-tests. The value of OCR should thereby have been evaluated more carefully as suggested. These assumptions had an impact on the outcome of the numerical analysis as the preconsolidation is a key parameter when modeling with the SS-model.

As seen in 3.2, the location of the boreholes from which the data is retrieved from is located at some distance from block E where the pile row of interest is located. As soil properties tends to vary, the distance from the borehole may have had an impact on the chosen parameters for the analysis.

There is always a complexity of modelling reality. This since many assumptions and simplifications must be made in order to scale down a problem from 3D to 2D as in this case. Those assumptions that might have influenced the deviation in the results in this case can be several. But the worthy to mention are, that modelling in plane strain will assume that the entire pile row is pushing equal amount of soil in one direction. No consideration have been given to interaction of displacements between the piles. When the effective radius was created, a simplification was made that the entire pile geometry became cylindrical. This will result in a different interaction between pile and soil in reality. The measurement point that the results have been compared with might have been exposed for other kinds of construction activities or damage allowing for some uncertainties in measurements. If there would have been more measurements in perpendicular direction from the pile row, the results from this study would have been easier to validate.

## 5.2 Limitations and further investigations

The tests that have been carried out for the project of scope are presented in table 3.1. No triaxial testing was performed on the soil which is necessary when using the SS-model as described in 2.5.3. This is a limitation in the analysis but it is also a limitation in Sweden in general where CRS testing is commonly performed only. Therefore the choice of using a more advanced material model should only be made if there is sufficient data and measurements. By only assuming empirical relations, the parameters used in the analysis are difficult to calibrate and validate. It should therefore be stated that more testing should be performed if representative results are to be pursued. This as the LE-model and MC-model is limited in predicting soil behaviour in comparison to other constitutive models.

The measurements from field could not validate which prediction method that encompasses the correct behaviour of soil. This since only one measurement point was considered in the horizontal direction perpendicular to the pile row. It would have been interesting to plot the deformations from field with the same distance as presented in the graphs in section 4.4. This would require several measure points carried out in the same direction with a given distance between the stations.

It should be noted that there are other methods that could be used for modelling piles in Plaxis 2D meaning that there is no recommended method to perform such an analysis, however the reason for the methods implemented in this thesis were that previous thesis and other research showed that they correspond well with measured data. However, the use of Line Displacement and Volume Expansion in this thesis might vary from other research as the size of the Line Displacement and the magnitude of the Volume Expansion is determined and expressed differently in comparison to others (see Appendix E). This might have affected the results from the numerical analysis in Plaxis 2D as both methods underestimate the vertical displacements and overestimates the horizontal displacements, see table 4.2. Another remark is that according to the sensitivity analysis the line displacement model did have a more even distribution of Seniscores compared to the Volume expansion model. This might confirm the statement made by Karstunen et al. (2017), that Line displacement is more stable from a numerical point of view. Therefore, it is humbly recommended that further research should focus on developing one numerical method that is considered useful for prediction of surrounding effects.

In order to present a multiplying factor, which was one of the objectives of this thesis, measurements in combination with logs of all the construction phases would have been required. A multiplying factor is therefore not recommended or presented in this thesis as the lack of this information is a great limitation. A more comprehensive research that accounts for the impact from: adjacent buildings, pre-existing foundations, the installed pile for the entire block and the different construction phases is necessary to perform in order to present a multiplying factor that could be used. However, it might not be possible to obtain such a factor using the simplified SSPM method only considering deformations at the ground surface (z=0). It should also be noted that SSPM only accounts for the pile being installed from the ground surface. In reality, there are many cases where the piles are installed from a depth which was the case in the project of scope in this thesis. One reason for the deviating results obtained from SSPM in comparison to the measurements is this limitation of SSPM. As the simplified method with z=0 is implemented in this thesis, it is difficult to predict the entire deformation situation. By conducting such an analysis accounting the deformations with depth, a more accurate estimation could have been obtained. This would also have required other measurement methods that are able to measure the deformations.

# 6
# Conclusion

It is clear that the SSPM simple pile is the best corresponding method towards the available measurements from field in this thesis. The method is also consistent in the investigated range of 150 meters. This as the deformations converges towards a value of zero at the considered distance.

However, it is of importance to understand the advantages and the drawbacks for the use of numerical simulation and the analytical calculation in different situations. The carried out analysis shows that none of them could dominate in terms of being accurate, time saving or cost beneficial. This study could not verify that the analytical prediction methods proposed by SSPM is accurate enough and the same statement implies for the numerical methods. In order to increase the accuracy of the numerical prediction methods, one should evaluate other material models that accounts for small strain stiffness and anisotropy in order to obtain the correct behaviour of soil. This involves the use of sufficient input data, that needs to be representative to the greatest extent in order to reflect reality. In practice, this puts a lot of responsibility on the practicing engineers and the contractors to demand and perform the necessary tests to provide useful information. The use of empirical relations can be used for a first estimation of a problem, but for accurate predictions it involves sources of error in the outcome.

By having all this, in combination with several case studies, meticulous measuring on site and experience among engineers, accurate predictions regarding surrounding effects from piles can be obtained. The same process implies for increasing the accuracy and the usability for an analytical prediction method, the only difference lies in the approach.

# References

Ahlén, C. (2009). *Pile Foundations – Short Handbook.*

Baligh, M. M. (1985). Strain Path Method. *Journal of Geotechnical Engineering*, *111*(9), 1108–1136.

Brinkgreve, R. (2002). Version 8 Material Models Manual. *Plaxis*, 1–146.

Brinkgreve, R., Engin, E., & Swolfs, W. (2017). Plaxis 2d manual. *Rotterdam, Netherlands, Balkema.*

Brinkgreve, R., Swolfs, W., & Engin, E. (2011). Plaxis 2d reference manual. *Delft University of Technology and PLAXIS bv The Netherlands.*

Castro, J., & Karstunen, M. (2010). Numerical simulations of stone column installation. *Canadian Geotechnical Journal*, *47*(10), 1127–1138. doi: 10.1139/t10-019

Dijkstra, J., Broere, W., & Heeres, O. M. (2011). Numerical simulation of pile installation. *Computers and Geotechnics*, *38*(5), 612–622. doi: 10.1016/j.compgeo.2011.04.004

Edstam, T., & Kullingsjö, A. (2011). Ground displacements due to pile driving in Gothenburg clay. *Numerical Methods in Geotechnical Engineering*, 625–630. doi: 10.1201/b10551-114

Hagerty, D. J., & Peck, R. B. (1971). Heave and lateral movements due to pile driving. *Journal of Soil Mechanics & Foundations Div.*

Jia, J. (2018). *Soil dynamics and foundation modeling.* Springer.

Karstunen, M., Amavasai, A., & Karlsson, M. (2017). *BEST SOIL : Soft Soil modelling and parameter determination* (No. November).

Knappett, J., & Craig, R. F. (2012). *Craig's soil mechanics.* CRC press.

Olsson, C., & Holm, G. (1993). *Påltyper .pdf.* Stockholm: Tryckeri Balder AB, Stockholm 1993.

Olsson, M. (2010). Calculating long-term settlement in soft clays. , 111.

Persson, M., & Stevens, R. (2012). *Kvickleremodellering Förutsägelser och tillämpning* (Tech. Rep.). Göteborgs Universitet Institutionen för geovetenskaper.

Potts, D., Zdravkovic, L., & Zdravković, L. (2001). *Finite element analysis in geotechnical engineering: Application.* Thomas Telford. Retrieved from `https://books.google.se/books?id=37PStsDpevoC`

Sagaseta, C., Whittle, A. J., & Santagata, M. (1997). Deformation analysis of shallow penetration in clay. *International Journal for Numerical and Analytical Methods in Geomechanics*, *21*(10), 687–719. doi: 10.1002/(SICI)1096-9853(199710)21:10<687::AID-NAG897>3.0.CO;2-3

Tjie-liong, G. (2015). Common Mistakes on the Application of Plaxis 2D in. *International Journal of Applied Engineering Research*(January 2014).

Viggiani, C., Mandolini, A., & Russo, G. (2012). *Piles and Pile Groups.* Retrieved from `http://doi.wiley.com/10.1002/9780470168097.ch8` doi: 10.1002/9780470168097.ch8

Wersäll, C., & Massarsch, K. R. (2013). Soil heave due to pile driving in clay. In *Sound geotechnical research to practice: Honoring robert d. holtz ii* (pp. 480–498).

Zeevaert, L. (1983). *Foundation engineering for difficult subsoil conditions.* New York : Nostrand Reinhold, cop. 1983. Retrieved from `http://proxy.lib.chalmers.se/login?url=http://search.ebscohost.com/login.aspx?direct=true&db=cat06296a&AN=clc.b1012351&lang=sv&site=eds-live&scope=site`

# A

# Appendix - Study Area

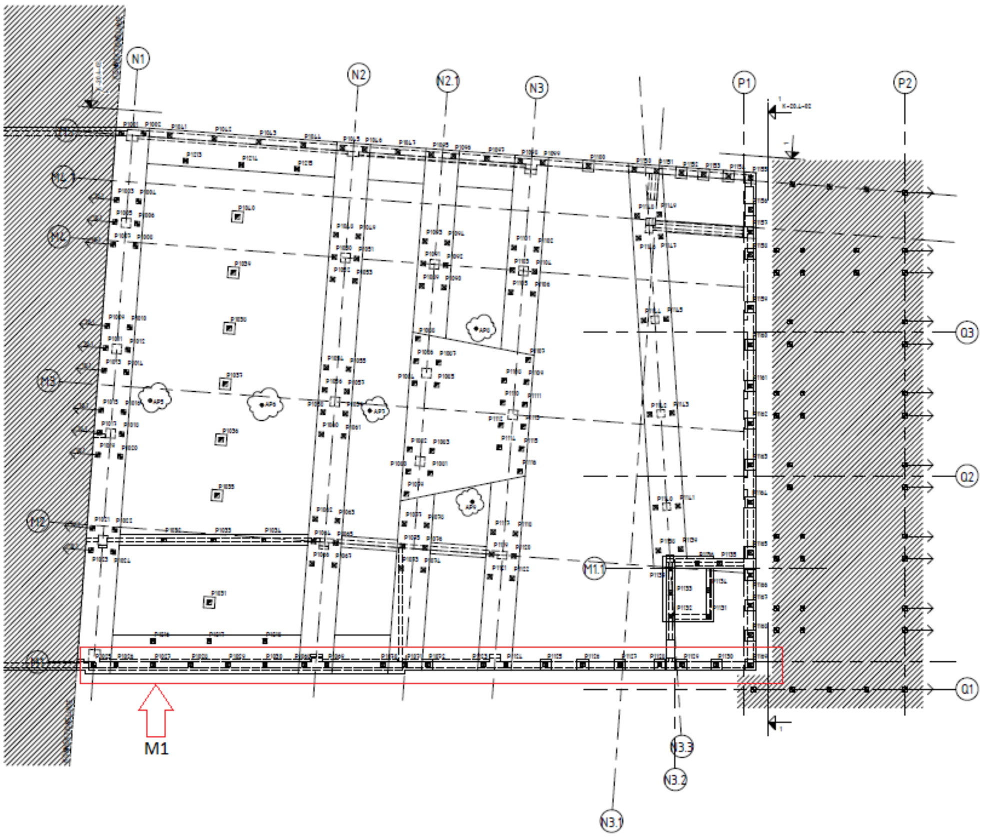


**Figure A.1:** Detailed view of section for block E where the exact pile location of row M1 can be found.

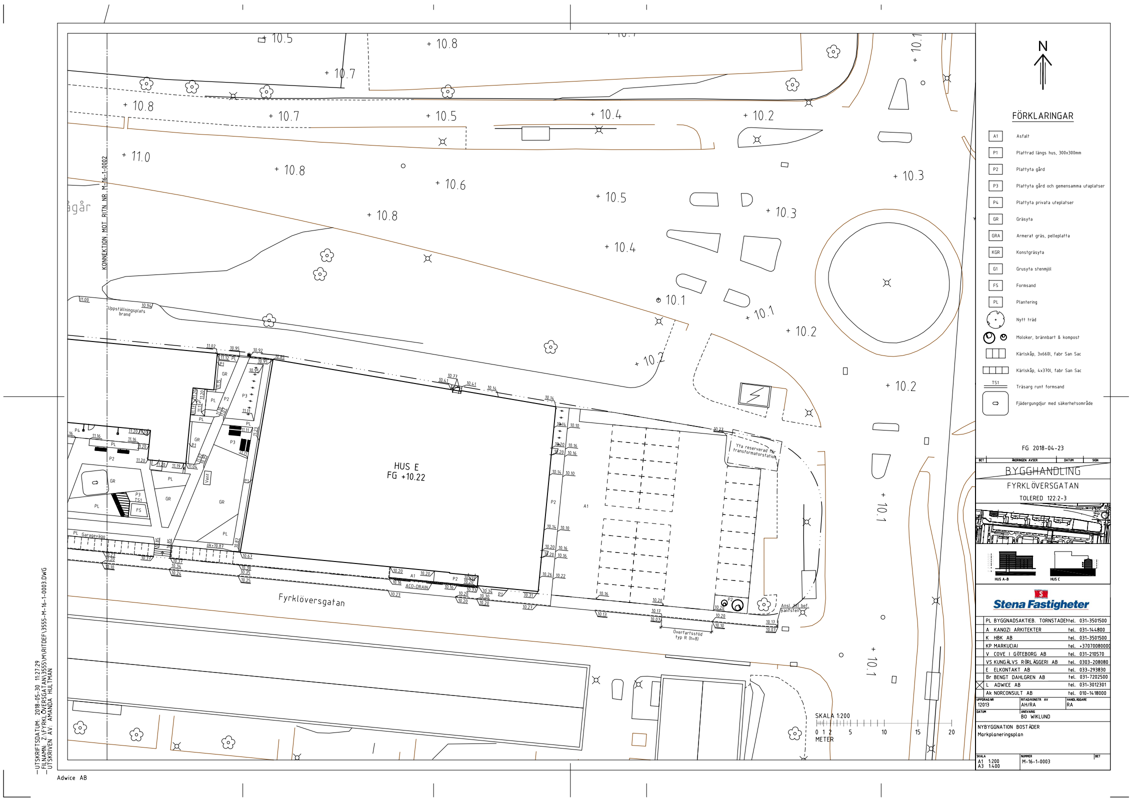


**Figure A.2:** Overview of a part of the construction area.

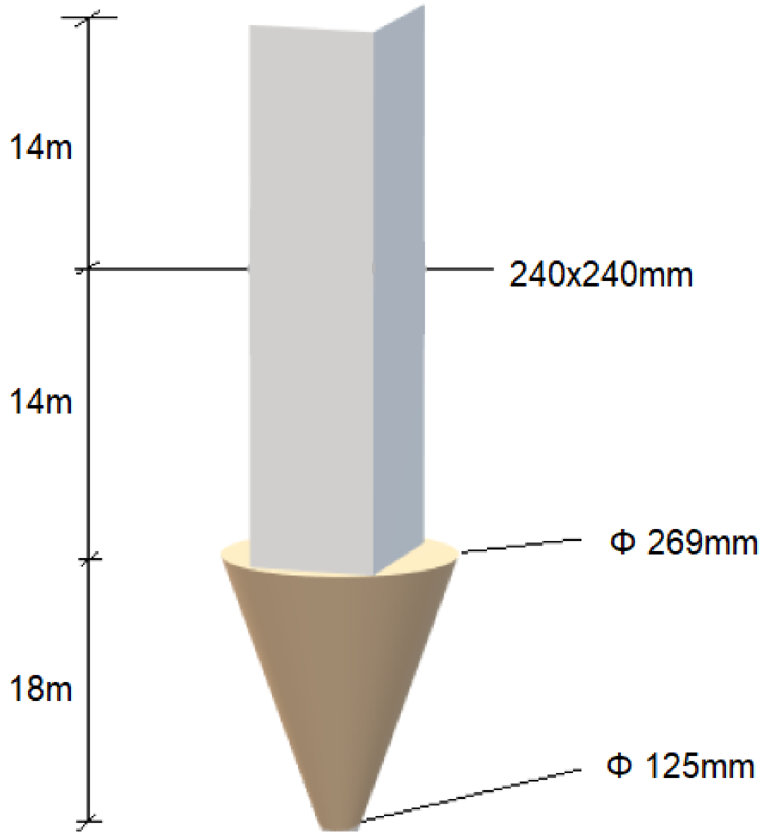


**Figure A.3:** View of the combined pile type that is used in the area (not made to scale).

The combination piles consist of concrete and wood. The schematic figure above visualizes their look and illustrates the geometric shape. The volume of one pile was calculated by first calculating the volume of the concrete part:
$0,24 \cdot 0,24 \cdot 28 = 1,61 m^3$.
For the wooden part an average diameter was calculated $(0,269+0,125)/2 = 0,197m$ and then it was considered as a cylinder with the volume:
$\pi \cdot (0,197/2)^2 = 0,549 m^3$.
Total volume of one pile $= 1,61 + 0,549 = 2,16 m^3$

The whole pile was transformed to a single cylindrical pile by considering the total volume and the length in order to obtain an effective radius $R = \sqrt{V/(\pi \cdot L)}$. In this case the obtained $R = \sqrt{2,16/(\pi \cdot 46)} \approx 0,12m$.

# B

# Appendix - Soil parameters

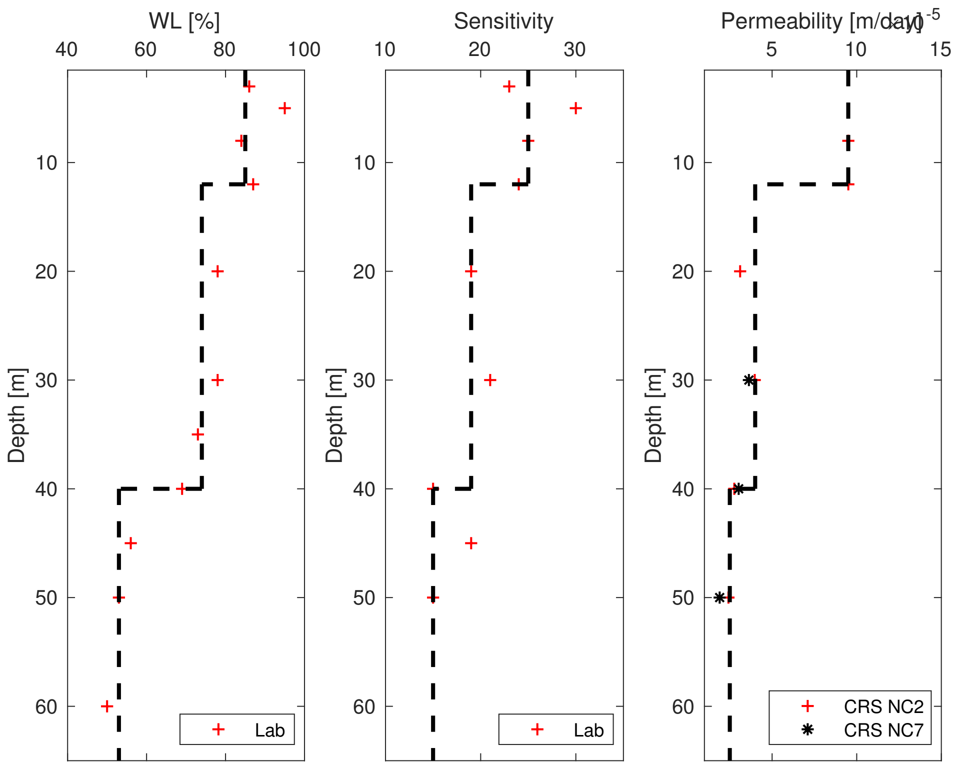


**Figure B.1:** Liquid limit, sensitivity and permeability.

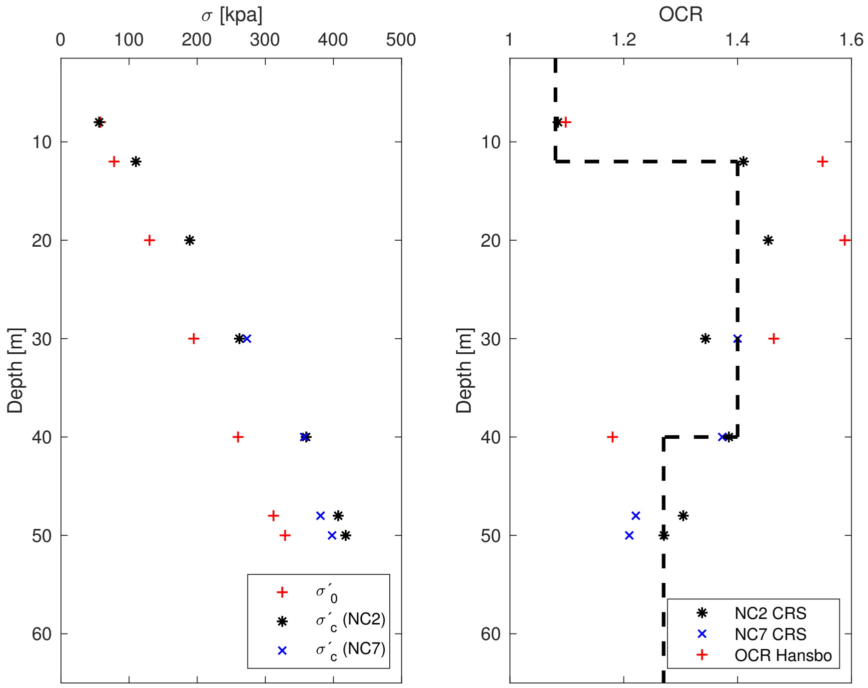


**Figure B.2:** Insitu-stress, preconsolidation pressure and OCR.

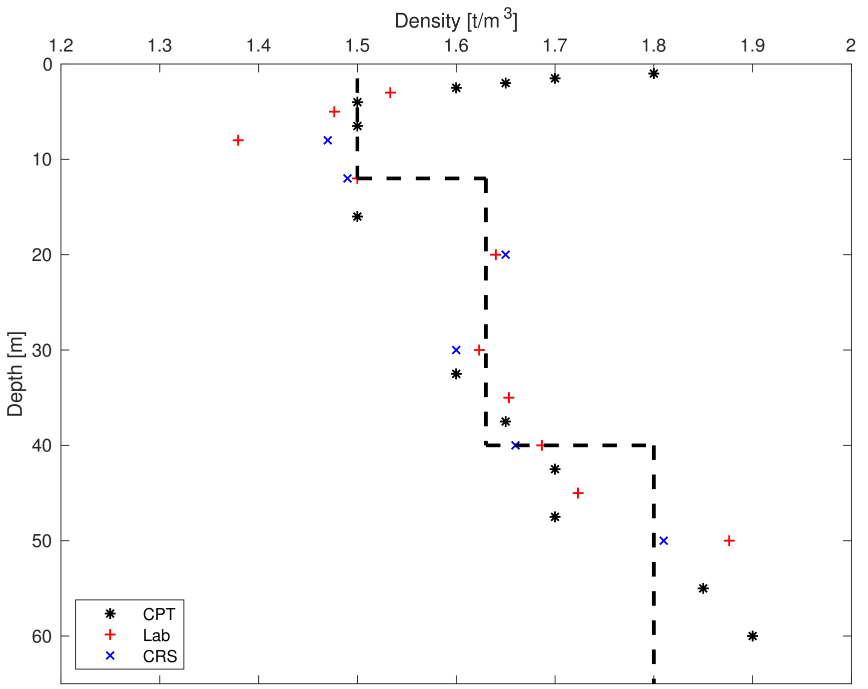


**Figure B.3:** Density of soil.

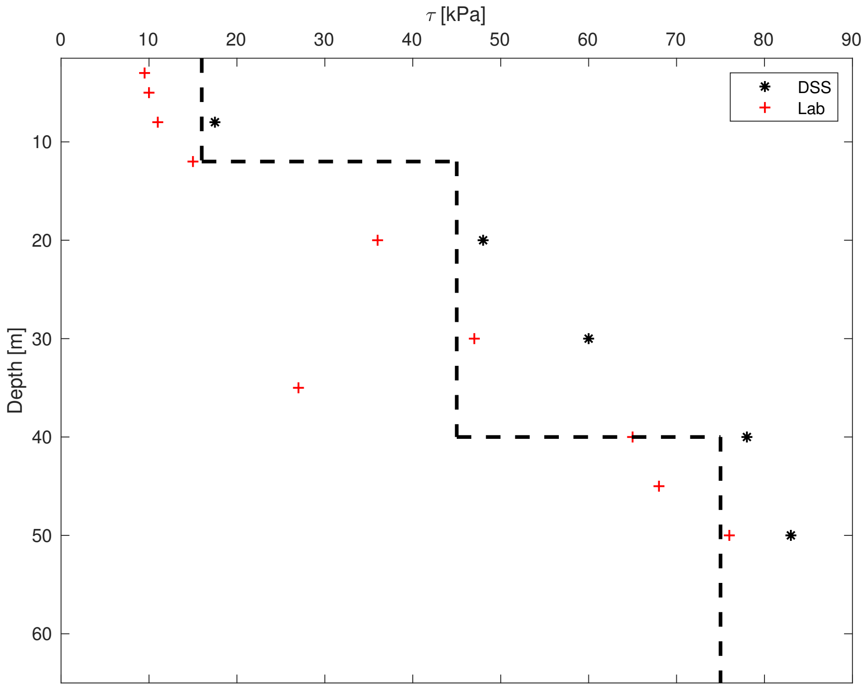


**Figure B.4:** Undrained shear strength.

# C

# Appendix - Calibration with SoilTest in Plaxis 2D

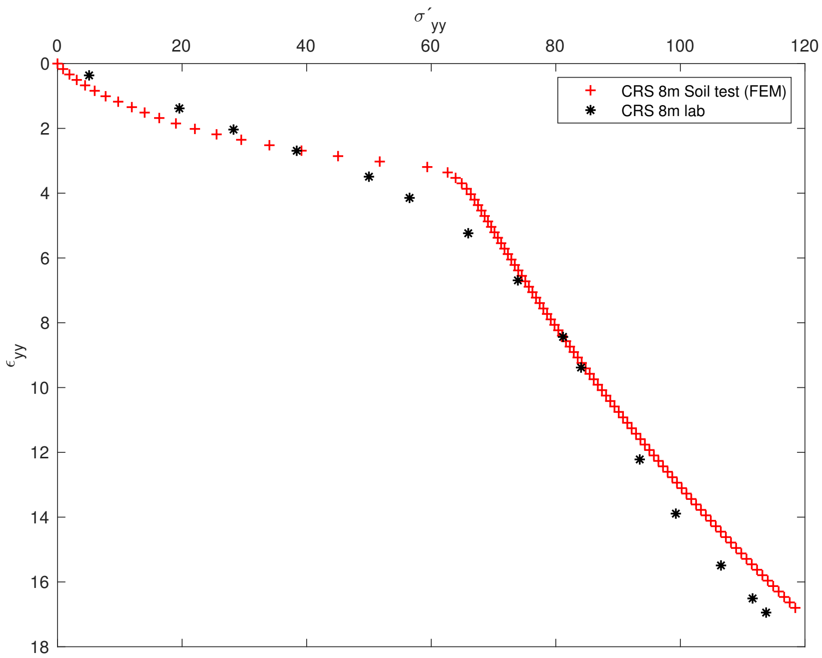


**Figure C.1:** CRS from SoilTest vs CRS from lab at 8 meters of depth(Borehole NC2).

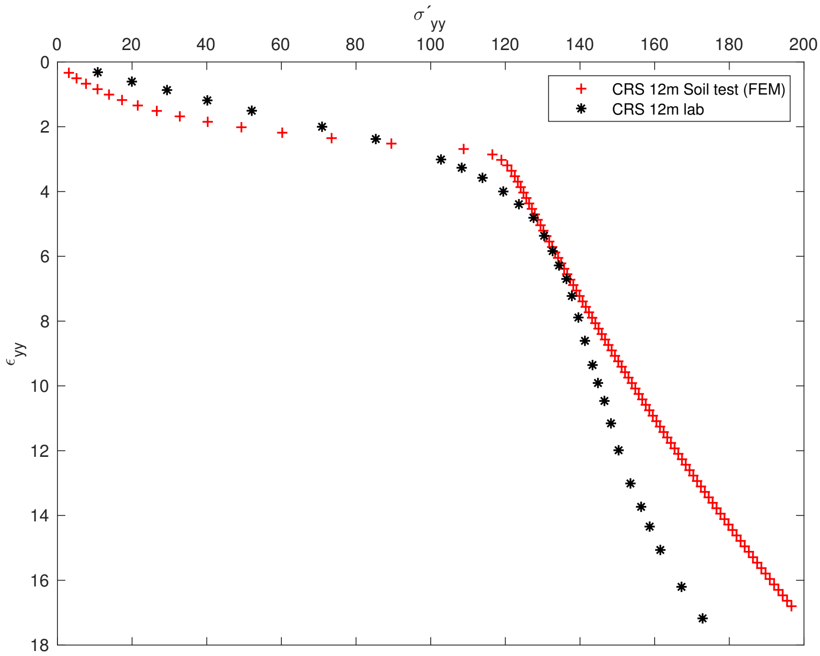


**Figure C.2:** CRS from SoilTest vs CRS from lab at 12 meters of depth(Borehole NC2).

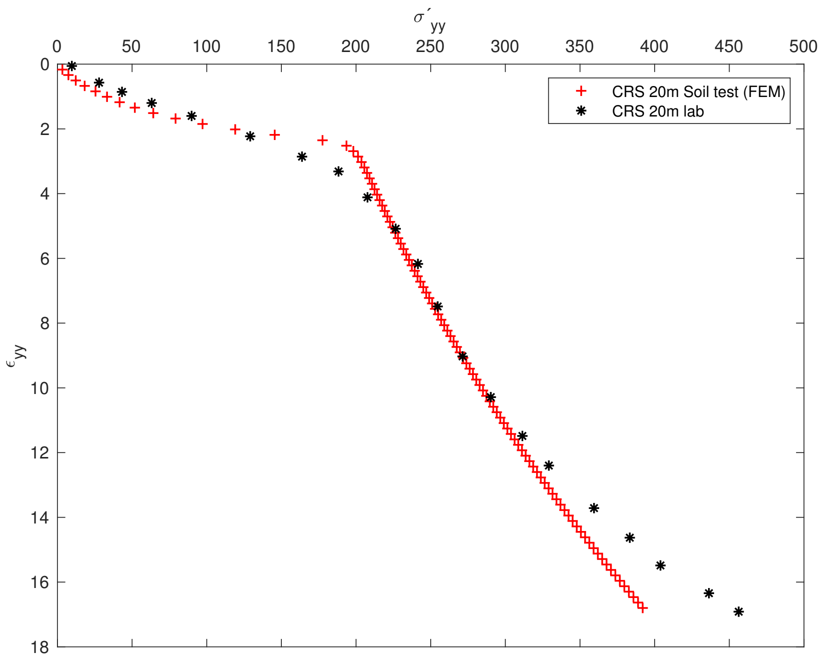


**Figure C.3:** CRS from SoilTest vs CRS from lab at 20 meters of depth(Borehole NC2).

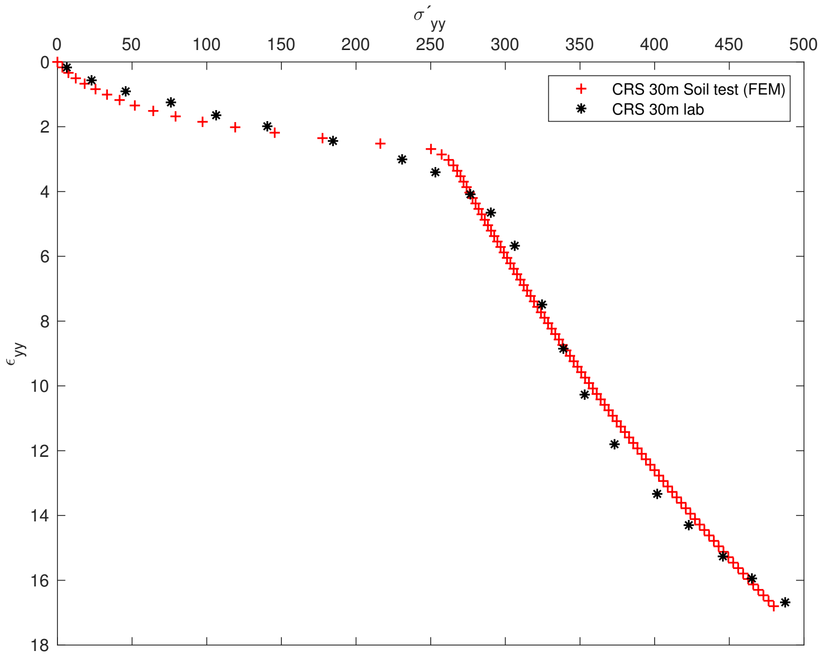


**Figure C.4:** CRS from SoilTest vs CRS from lab at 30 meters of depth (Borehole NC2).

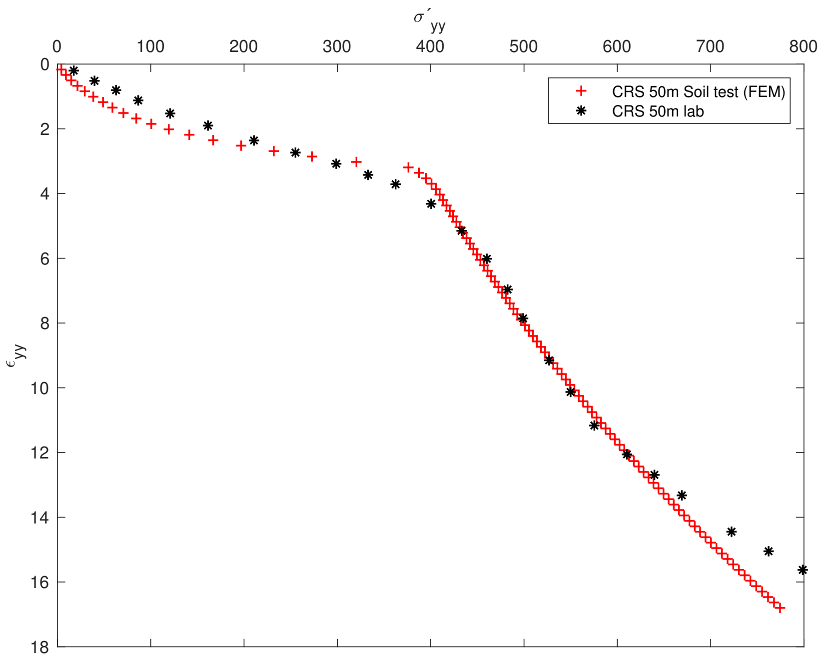


**Figure C.5:** CRS from SoilTest vs CRS from lab at 50 meters of depth (Borehole NC7) .

# D

# Appendix - Plaxis figures

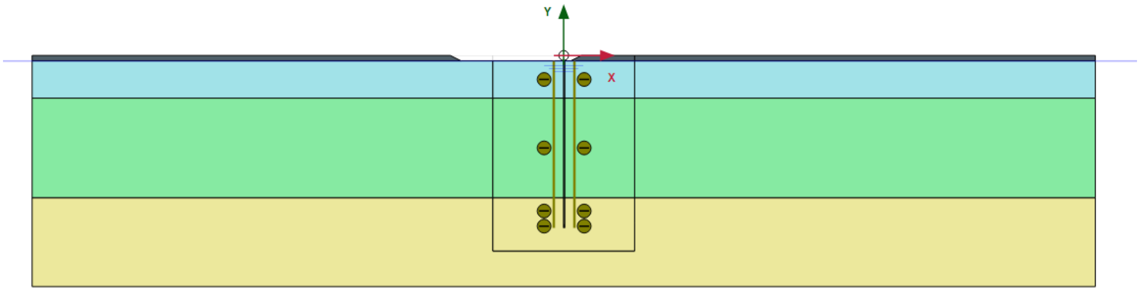


**Figure D.1:** View of the model initiated with the volume expansion method.

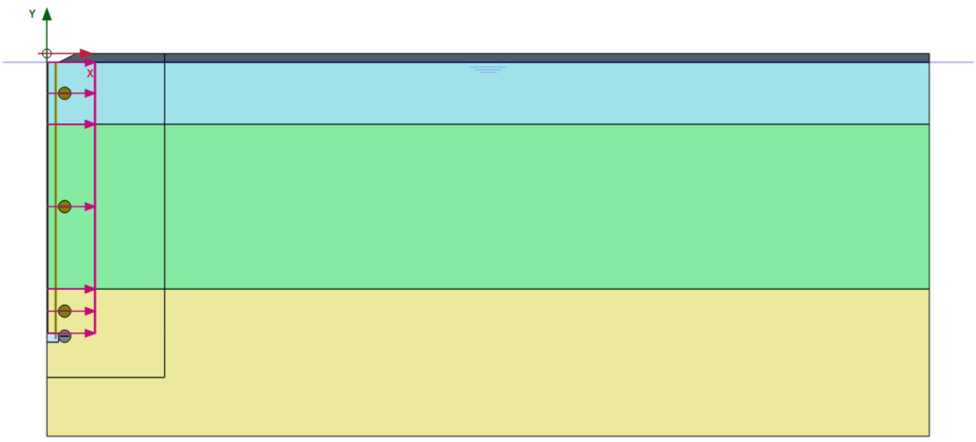


**Figure D.2:** View of the model initiated with the line displacement method.

# E

# Appendix - Calculations

Length of piling area: 14,57m
Width of piling area: 0,24m
Depth of piling area: 46m
Volume of soil in the piling area (pile row): $14,57m \cdot 0,24m \cdot 46m = 160,85m^3$

Volume of one pile: $2,09m^3$
Volume of seven piles: $7 \cdot 2,09m^3 = 14,66m^3$

Total volume in piling area when piles are installed: $160,85 + 14,66 = 175,51m^3$
New width of piling area $= 175,51/(46 \cdot 14,57) = 0,2618m$

**Prescribed-displacement** $= (0,2618 - 0,24)/2 = 0,0109m$ in x-direction since the change of volume was distributed over the width.

**Volume expansion** $= (0,2618 - 0,24)/0,24 = 0,091(9,1\%)$ volume increase for $\varepsilon_x$ since the change of volume was distributed over the width.

**Simple wall SSPM**:
w $= 14,66/46 \cdot 14,57 = 0,0218$
L=46m

The Simple wall width (w) was based on the same value of the prescribed line displacement. This in order to make the both methods comparable, since it is assumed that the volume of the pile row is the cause of displacements.

# F

# Appendix - Sensitivity Analysis Line Displacement

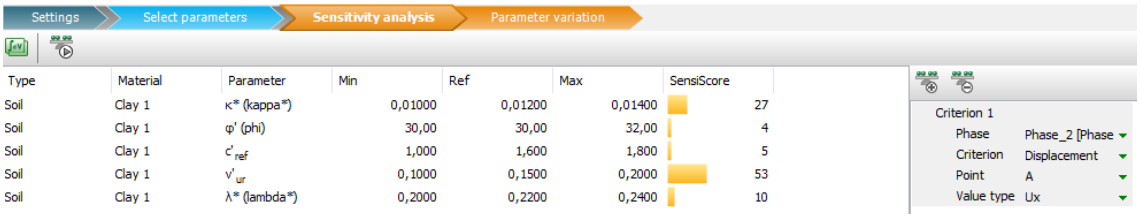


| Type | Material | Parameter | Min | Ref | Max | SensiScore |
|---|---|---|---|---|---|---|
| Soil | Clay 1 | κ* (kappa*) | 0,01000 | 0,01200 | 0,01400 | 27 |
| Soil | Clay 1 | φ' (phi) | 30,00 | 30,00 | 32,00 | 4 |
| Soil | Clay 1 | $c'_{ref}$ | 1,000 | 1,600 | 1,800 | 5 |
| Soil | Clay 1 | $\nu'_{ur}$ | 0,1000 | 0,1500 | 0,2000 | 53 |
| Soil | Clay 1 | λ* (lambda*) | 0,2000 | 0,2200 | 0,2400 | 10 |

**Figure F.1:** SensiScore given to different parameters for Clay 1 with respect to Horizontal displacement, in model where the **Line displacement** where initiated.

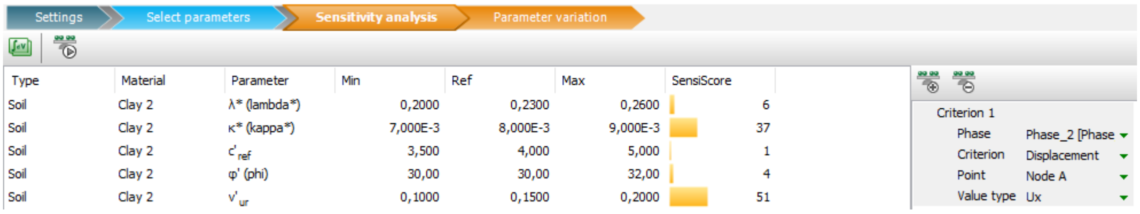


| Type | Material | Parameter | Min | Ref | Max | SensiScore |
|---|---|---|---|---|---|---|
| Soil | Clay 2 | λ* (lambda*) | 0,2000 | 0,2300 | 0,2600 | 6 |
| Soil | Clay 2 | κ* (kappa*) | 7,000E-3 | 8,000E-3 | 9,000E-3 | 37 |
| Soil | Clay 2 | $c'_{ref}$ | 3,500 | 4,000 | 5,000 | 1 |
| Soil | Clay 2 | φ' (phi) | 30,00 | 30,00 | 32,00 | 4 |
| Soil | Clay 2 | $\nu'_{ur}$ | 0,1000 | 0,1500 | 0,2000 | 51 |

**Figure F.2:** SensiScore given to different parameters for Clay 2 with respect to Horizontal displacement, in model where the **Line displacement** where initiated.

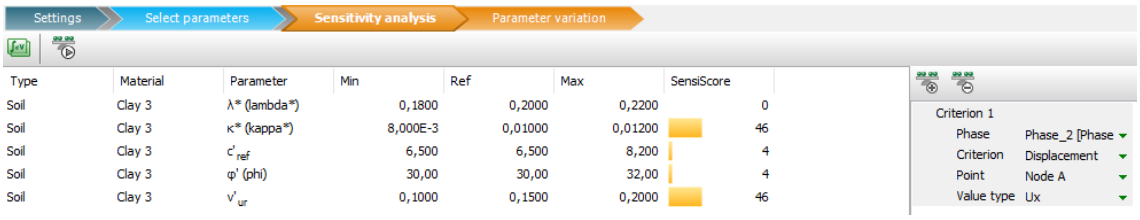


| Type | Material | Parameter | Min | Ref | Max | SensiScore |
|---|---|---|---|---|---|---|
| Soil | Clay 3 | λ* (lambda*) | 0,1800 | 0,2000 | 0,2200 | 0 |
| Soil | Clay 3 | κ* (kappa*) | 8,000E-3 | 0,01000 | 0,01200 | 46 |
| Soil | Clay 3 | $c'_{ref}$ | 6,500 | 6,500 | 8,200 | 4 |
| Soil | Clay 3 | φ' (phi) | 30,00 | 30,00 | 32,00 | 4 |
| Soil | Clay 3 | $\nu'_{ur}$ | 0,1000 | 0,1500 | 0,2000 | 46 |

**Figure F.3:** SensiScore given to different parameters for Clay 3 with respect to Horizontal displacement, in model where the **Line displacement** where initiated.

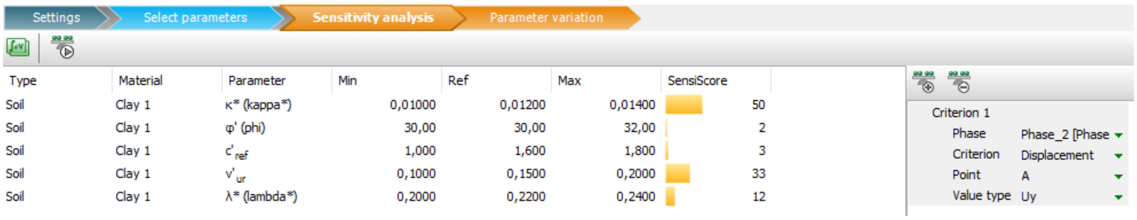


| Type | Material | Parameter | Min | Ref | Max | SensiScore |
|---|---|---|---|---|---|---|
| Soil | Clay 1 | κ* (kappa*) | 0,01000 | 0,01200 | 0,01400 | 50 |
| Soil | Clay 1 | φ' (phi) | 30,00 | 30,00 | 32,00 | 2 |
| Soil | Clay 1 | $c'_{ref}$ | 1,000 | 1,600 | 1,800 | 3 |
| Soil | Clay 1 | $\nu'_{ur}$ | 0,1000 | 0,1500 | 0,2000 | 33 |
| Soil | Clay 1 | λ* (lambda*) | 0,2000 | 0,2200 | 0,2400 | 12 |

**Figure F.4:** SensiScore given to different parameters for Clay 1 with respect to Vertical displacement, in model where the **Line displacement** where initiated.

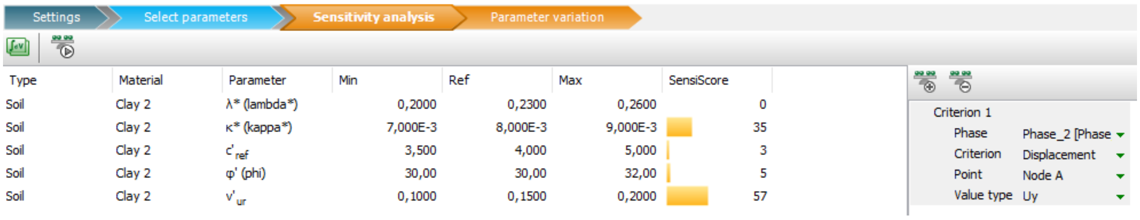


| Type | Material | Parameter | Min | Ref | Max | SensiScore |
|---|---|---|---|---|---|---|
| Soil | Clay 2 | λ* (lambda*) | 0,2000 | 0,2300 | 0,2600 | 0 |
| Soil | Clay 2 | κ* (kappa*) | 7,000E-3 | 8,000E-3 | 9,000E-3 | 35 |
| Soil | Clay 2 | $c'_{ref}$ | 3,500 | 4,000 | 5,000 | 3 |
| Soil | Clay 2 | φ' (phi) | 30,00 | 30,00 | 32,00 | 5 |
| Soil | Clay 2 | $\nu'_{ur}$ | 0,1000 | 0,1500 | 0,2000 | 57 |

**Figure F.5:** SensiScore given to different parameters for Clay 2 with respect to Vertical displacement, in model where the **Line displacement** where initiated.

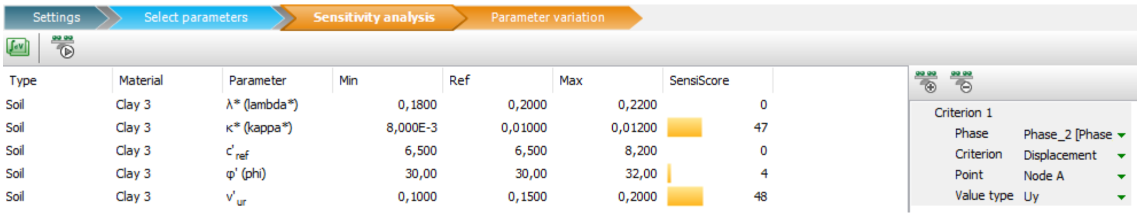


| Type | Material | Parameter | Min | Ref | Max | SensiScore |
|---|---|---|---|---|---|---|
| Soil | Clay 3 | λ* (lambda*) | 0,1800 | 0,2000 | 0,2200 | 0 |
| Soil | Clay 3 | κ* (kappa*) | 8,000E-3 | 0,01000 | 0,01200 | 47 |
| Soil | Clay 3 | $c'_{ref}$ | 6,500 | 6,500 | 8,200 | 0 |
| Soil | Clay 3 | φ' (phi) | 30,00 | 30,00 | 32,00 | 4 |
| Soil | Clay 3 | $\nu'_{ur}$ | 0,1000 | 0,1500 | 0,2000 | 48 |

**Figure F.6:** SensiScore given to different parameters for Clay 3 with respect to Vertical displacement, in model where the **Line displacement** where initiated.

# G

# Appendix - Sensitivity Analysis Volume Expansion

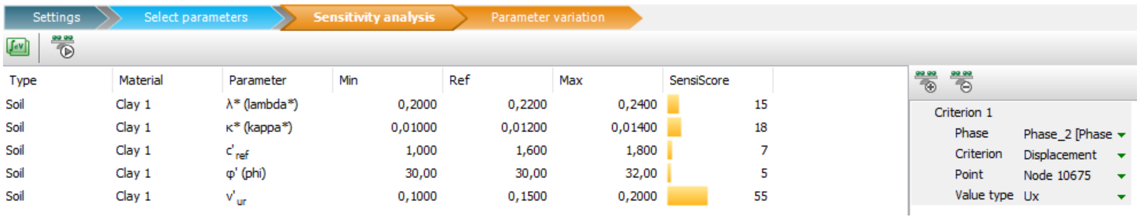

| Type | Material | Parameter | Min | Ref | Max | SensiScore |
|---|---|---|---|---|---|---|
| Soil | Clay 1 | λ* (lambda*) | 0,2000 | 0,2200 | 0,2400 | 15 |
| Soil | Clay 1 | κ* (kappa*) | 0,01000 | 0,01200 | 0,01400 | 18 |
| Soil | Clay 1 | $c'_{ref}$ | 1,000 | 1,600 | 1,800 | 7 |
| Soil | Clay 1 | φ' (phi) | 30,00 | 30,00 | 32,00 | 5 |
| Soil | Clay 1 | $\nu'_{ur}$ | 0,1000 | 0,1500 | 0,2000 | 55 |



**Figure G.1:** SensiScore given to different parameters for Clay 1 with respect to Horizontal displacement, in model where the **Volume Expansion** where initiated.

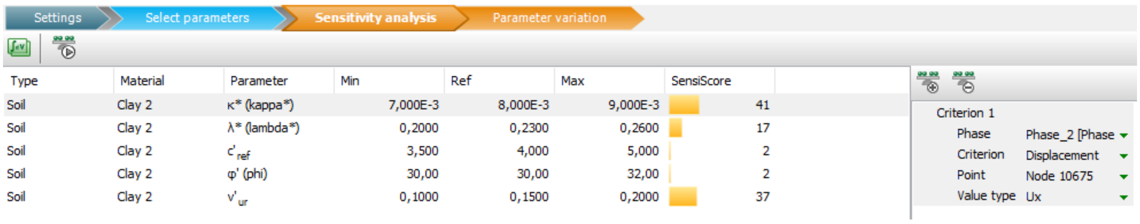

| Type | Material | Parameter | Min | Ref | Max | SensiScore |
|---|---|---|---|---|---|---|
| Soil | Clay 2 | κ* (kappa*) | 7,000E-3 | 8,000E-3 | 9,000E-3 | 41 |
| Soil | Clay 2 | λ* (lambda*) | 0,2000 | 0,2300 | 0,2600 | 17 |
| Soil | Clay 2 | $c'_{ref}$ | 3,500 | 4,000 | 5,000 | 2 |
| Soil | Clay 2 | φ' (phi) | 30,00 | 30,00 | 32,00 | 2 |
| Soil | Clay 2 | $\nu'_{ur}$ | 0,1000 | 0,1500 | 0,2000 | 37 |



**Figure G.2:** SensiScore given to different parameters for Clay 2 with respect to Horizontal displacement, in model where the **Volume Expansion** where initiated.

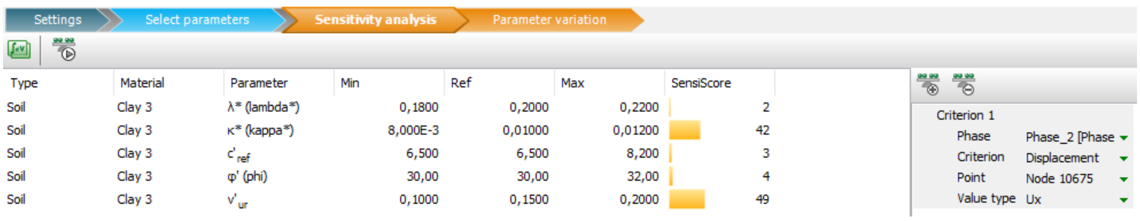

| Type | Material | Parameter | Min | Ref | Max | SensiScore |
|---|---|---|---|---|---|---|
| Soil | Clay 3 | λ* (lambda*) | 0,1800 | 0,2000 | 0,2200 | 2 |
| Soil | Clay 3 | κ* (kappa*) | 8,000E-3 | 0,01000 | 0,01200 | 42 |
| Soil | Clay 3 | $c'_{ref}$ | 6,500 | 6,500 | 8,200 | 3 |
| Soil | Clay 3 | φ' (phi) | 30,00 | 30,00 | 32,00 | 4 |
| Soil | Clay 3 | $\nu'_{ur}$ | 0,1000 | 0,1500 | 0,2000 | 49 |



**Figure G.3:** SensiScore given to different parameters for Clay 3 with respect to Horizontal displacement, in model where the **Volume Expansion** where initiated.

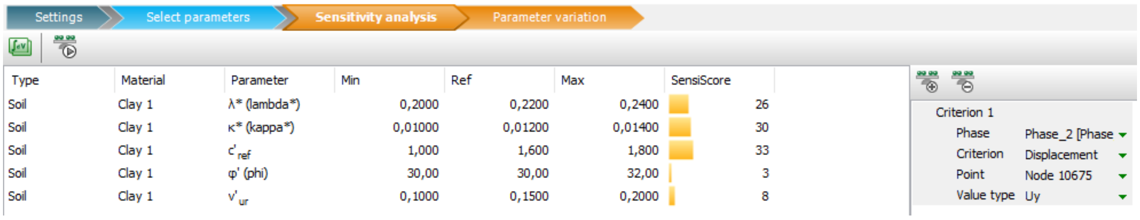


| Type | Material | Parameter | Min | Ref | Max | SensiScore |
|---|---|---|---|---|---|---|
| Soil | Clay 1 | λ* (lambda*) | 0,2000 | 0,2200 | 0,2400 | 26 |
| Soil | Clay 1 | κ* (kappa*) | 0,01000 | 0,01200 | 0,01400 | 30 |
| Soil | Clay 1 | $c'_{ref}$ | 1,000 | 1,600 | 1,800 | 33 |
| Soil | Clay 1 | φ' (phi) | 30,00 | 30,00 | 32,00 | 3 |
| Soil | Clay 1 | $\nu'_{ur}$ | 0,1000 | 0,1500 | 0,2000 | 8 |

**Figure G.4:** SensiScore given to different parameters for Clay 1 with respect to Vertical displacement, in model where the **Volume Expansion** where initiated.

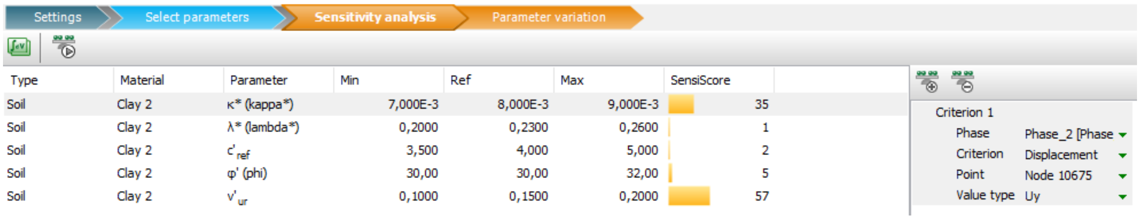


| Type | Material | Parameter | Min | Ref | Max | SensiScore |
|---|---|---|---|---|---|---|
| Soil | Clay 2 | κ* (kappa*) | 7,000E-3 | 8,000E-3 | 9,000E-3 | 35 |
| Soil | Clay 2 | λ* (lambda*) | 0,2000 | 0,2300 | 0,2600 | 1 |
| Soil | Clay 2 | $c'_{ref}$ | 3,500 | 4,000 | 5,000 | 2 |
| Soil | Clay 2 | φ' (phi) | 30,00 | 30,00 | 32,00 | 5 |
| Soil | Clay 2 | $\nu'_{ur}$ | 0,1000 | 0,1500 | 0,2000 | 57 |

**Figure G.5:** SensiScore given to different parameters for Clay 2 with respect to Vertical displacement, in model where the **Volume Expansion** where initiated.

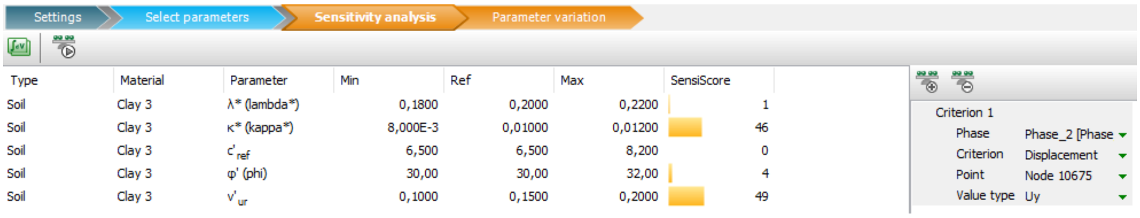


| Type | Material | Parameter | Min | Ref | Max | SensiScore |
|---|---|---|---|---|---|---|
| Soil | Clay 3 | λ* (lambda*) | 0,1800 | 0,2000 | 0,2200 | 1 |
| Soil | Clay 3 | κ* (kappa*) | 8,000E-3 | 0,01000 | 0,01200 | 46 |
| Soil | Clay 3 | $c'_{ref}$ | 6,500 | 6,500 | 8,200 | 0 |
| Soil | Clay 3 | φ' (phi) | 30,00 | 30,00 | 32,00 | 4 |
| Soil | Clay 3 | $\nu'_{ur}$ | 0,1000 | 0,1500 | 0,2000 | 49 |

**Figure G.6:** SensiScore given to different parameters for Clay 3 with respect to Vertical displacement, in model where the **Volume Expansion** where initiated.